Carbon dioxide fluxes increase from day to night across European streams

Katrin Attermeyer[1,2,3], Joan Pere Casas-Ruiz[4,5], Thomas Fuss[6], Ada Pastor[4,5,7], Sophie Cauvy-Fraunié[8], Danny Sheath[9,10], Anna C. Nydahl[1], Alberto Doretto[11,12], Ana Paula Portela[13,14], Brian C. Doyle[15], Nikolay Simov[16], Catherine Gutmann Roberts[9], Georg H. Niedrist[17], Xisca Timoner[4,5], Vesela Evtimova[18], Laura Barral-Fraga[5], Tea Bašić[9,19], Joachim Audet[20,21], Anne Deininger[22,23], Georgina Busst[9], Stefano Fenoglio[12,24], Núria Catalán[4,5,25], Elvira de Eyto[26], Francesca Pilotto[22,27], Jordi-René Mor[4,28], Juliana Monteiro[29], David Fletcher[9], Christian Noss[30], Miriam Colls[4,5], Magdalena Nagler[31], Liu Liu[30,32], Clara Romero González-Quijano[33], Ferran Romero[4,5], Nina Pansch[32], José L. J. Ledesma[20,34,35], Josephine Pegg[9,36], Marcus Klaus[22,37], Anna Freixa[4,5], Sonia Herrero Ortega[32], Clara Mendoza-Lera[8,30], Adam Bednařík[38,39], Jérémy A. Fonvielle[32], Peter J. Gilbert[40], Lyubomir A. Kenderov[41], Martin Rulík[38], Pascal Bodmer[30,42,43]*

1 Limnology/Department of Ecology and Genetics, Uppsala University, 75236 Uppsala, Sweden

2 WasserCluster Lunz – Biologische Station, 3293 Lunz am See, Austria

3 Department of Functional and Evolutionary Ecology, University of Vienna, 1090 Vienna, Austria

4 Catalan Institute for Water Research (ICRA), 17003 Girona, Spain

5 Department of Environmental Sciences, University of Girona (UdG), 17003 Girona, Spain

6 Fluvial Ecosystem Ecology, Department of Ecology, University of Innsbruck, 6020 Innsbruck, Austria

7 present address: Department of Biology, Aarhus University, 8000 Aarhus C, Denmark

8 INRAE, UR Riverly, Centre de Lyon-Villeurbanne, Villeurbanne Cedex, France

9 Department of Life and Environmental Sciences, Bournemouth University, BH12 5BB, UK

10 present address: Institute of Global Health, Faculty of Medicine, University of Geneva, Campus Biotech, 1211 Geneva, Switzerland

11 Department of Sciences and Technological Innovation, University of Piemonte Orientale, 15121 Alessandria, Italy

12 ALPSTREAM – Alpine Stream Research Center, 12030 Ostana, Italy

13 Research Centre in Biodiversity and Genetic Resources (CIBIO-InBIO), University of Porto, 4485-661 Vila do Conde, Portugal

14 Faculty of Sciences, University of Porto, 4169-007 Porto, Portugal

15 Centre for Freshwater and Environmental Studies, Dundalk Institute of Technology, Dundalk, Co Louth, A91 K584, Ireland

16 National Museum of Natural History, Bulgarian Academy of Sciences, 1000 Sofia, Bulgaria

17 River and Conservation Research, Department of Ecology, University of Innsbruck, 6020 Innsbruck, Austria

18 Department of Aquatic Ecosystems, Institute of Biodiversity and Ecosystem Research, Bulgarian Academy of Sciences, 1000 Sofia, Bulgaria

19 present address: Centre for Environment, Fisheries and Aquaculture Science (Cefas), Pakefield Road, Lowestoft, Suffolk NR33 OHT, UK

20 Department of Aquatic Sciences and Assessment, Swedish University of Agricultural Sciences, 75007 Uppsala, Sweden

21 present address: Department of Bioscience, Aarhus University, 8600 Silkeborg, Denmark

22 Department of Ecology and Environmental Science, Umeå University, 90736 Umeå, Sweden

23 present address: Norwegian Institute for Water Research, 0349 Oslo, Norway

24 Department of Life Sciences and Systems Biology, University of Turin, 10124 Turin, Italy

25 present address: Laboratoire des Sciences du Climat et de l'Environnement (LSCE), CEA, CNRS, UVSQ, 91191 Gif-Sur-Yvette, France / United States Geological Survey, Boulder, CO 80303, USA

26 Marine Institute, Furnace, Newport, Co Mayo F28 PF65, Ireland

27 present address: Environmental Archaeology Lab, Department of Historical, Philosophical and Religious studies, Umeå University, 90736 Umeå, Sweden

28 Department of Evolutionary Biology, Ecology and Environmental Sciences, Faculty of Biology, University of Barcelona (UB), 08028 Barcelona, Spain

29 Centre for Ecology, Evolution and Environmental Changes (cE3c), Faculdade de Ciências, Universidade de Lisboa, 1749-016 Lisboa, Portugal

30 Institute for Environmental Sciences, University of Koblenz-Landau, 76829 Landau, Germany

31 Institute of Microbiology, University of Innsbruck, 6020 Innsbruck, Austria

32 Experimental Limnology, Leibniz-Institute of Freshwater Ecology and Inland Fisheries (IGB), 16775 Stechlin, Germany

33 Ecohydrology, Leibniz-Institute of Freshwater Ecology and Inland Fisheries (IGB), 12587 Berlin, Germany

34 Center for Advanced Studies of Blanes, Spanish National Research Council, 17300 Blanes, Spain

35 Institute of Geography and Geoecology, Karlsruhe Institute of Technology, 76131 Karlsruhe, Germany

36 South African Institute of Aquatic Biodiversity, Makhanda, 6139, South Africa

37 present address: Department of Forest Ecology and Management, Swedish University of Agricultural Sciences, 90183 Umeå, Sweden

38 Department of Ecology and Environmental Sciences, Palacký University Olomouc, 77900 Olomouc, Czech Republic

39 present address: Global Change Research Institute of the Czech Academy of Sciences, 603 00 Brno, Czech Republic

40 Environmental Research Institute, University of Highlands and Islands (UHI), Thurso KW14 7JD, Scotland, UK

41 Department of General and Applied Hydrobiology, Sofia University "St. Kliment Ohridski", 1164 Sofia, Bulgaria

42 Chemical Analytics and Biogeochemistry, Leibniz-Institute of Freshwater Ecology and Inland Fisheries, 12587 Berlin, Germany

43 present address: Groupe de Recherche Interuniversitaire en Limnologie, Département des Sciences Biologiques, Université du Québec à Montréal, Montréal H3C 3J7, Canada

*Corresponding author: Katrin Attermeyer (katrin.attermeyer@univie.ac.at)

Author order except first, second, and last author was computed randomly

This paper is a non-peer reviewed preprint submitted to EarthArXiv. This preprint has been submitted to Nature Communications Earth and Environment for consideration for publication.

Abstract

Globally, inland waters emit over 2 Pg of carbon (C) per year as carbon dioxide (CO_2), of which the majority originates from streams and rivers. Despite the global significance of fluvial CO_2 emissions, little is known about their diel dynamics. We present the first large-scale assessment of day- and night-time CO_2 fluxes at the water-air interface across European streams. Fluxes were directly measured four times throughout one year using drifting chambers. Median CO_2 fluxes amounted to 1.4 and 2.1 mmol m^{-2} h^{-1} at midday and midnight, respectively, with night fluxes exceeding those during the day by 39%. Diel CO_2 flux variability was mainly attributed to changes in the water partial pressure of CO_2 (pCO_2) but no consistent drivers could be identified across sites. Our results highlight widespread day-night changes in fluvial CO_2 fluxes and that the time of day greatly influences measured CO_2 fluxes across European streams.

Introduction

Inland waters are important sources of atmospheric carbon dioxide (CO_2) partially offsetting the terrestrial carbon sink [1,2]. Streams and rivers therein represent major CO_2 emitters [3]. Fluvial CO_2 fluxes are primarily controlled by the gas exchange velocity at the water-air interface (k) and the gradient between the water and atmospheric partial pressures of CO_2 (pCO_2) [4]. Both parameters are highly variable in space and time [5,6], causing uncertainty in the magnitude of regional and global fluvial CO_2 emissions [2].

The high spatiotemporal variability of k and water pCO_2 can be attributed to a complex interplay of underlying controls. While k in streams is mostly driven by water turbulence created by variations in flow and stream morphology [7], the water pCO_2 is influenced by the degree of hydrological connectivity between the stream and the adjacent riparian soils [8] as well as by in-stream processes (e.g., stream metabolism). The supply of CO_2 from external sources, such as soil water or groundwater, into streams varies with reach and season [5,9]. Furthermore, seasonal and diel changes in stream pCO_2 are attributed to stream metabolism driven by temperature and solar radiation [10–13]. Ecosystem respiration, a source of CO_2 in the stream, takes place throughout the whole day, and gross primary production, a sink of CO_2, occurs only during daylight. Temperature and solar radiation also directly influence water pCO_2, the former by changing the solubility of the gas and the latter due to photomineralization [14]. However, questions remain regarding the magnitude and relative drivers of seasonal and diel fluctuations of CO_2 fluxes in streams.

Presently, most fluvial CO_2 emission values are derived from k estimates based on water velocity and stream channel slope and on water pCO_2 values indirectly calculated from alkalinity, pH, and temperature [3]. This approach fails to capture the high spatiotemporal variability observed for k and pCO_2 and therefore can provide imprecise estimates of CO_2 fluxes [15,16]. Direct field observations provide the means to improve estimates and understanding of the drivers behind spatiotemporal variability, and thus the dynamics of CO_2 outgassing from running waters. However, besides some local studies that indirectly infer CO_2 fluxes from pCO_2 concentrations and k [11,12,17,18], no direct measurements exist that compare day- and night-time CO_2 fluxes from streams on a larger spatial scale.

The aim of this study was to assess the magnitude and drivers of stream CO_2 flux variations between day and night across European streams. We hypothesized that CO_2 fluxes would differ between day and night due to diel variations in terrestrial inorganic carbon inputs, *in situ* metabolism, and temperature. As higher temperatures and solar radiation may drive differences in pCO_2, we expected a higher difference between day- and night-time fluxes with warmer temperatures and at lower latitudes. Hence, we measured day and night-time fluxes of CO_2 at four different periods throughout one year from 34 streams (Strahler stream orders from 1 to 6) in 11 countries across Europe following a standardized procedure. CO_2 fluxes were measured starting at midday (11am Greenwich Mean Time (GMT)) and midnight (11pm GMT) with drifting flux chambers equipped with CO_2 sensors as described in Bastviken et al. (2015) [19]. In the majority of the European streams, we found increased CO_2 fluxes at the water-air interface in the night compared to the day with a median increase of 0.5 mmol m^{-2} h^{-1}. Most of the observed CO_2 flux variability was explained by changes in pCO_2 from day to night with more pronounced changes at lower latitudes.

Results and Discussion

Magnitude of CO_2 flux variation from day to night

Midday CO_2 fluxes at the water-air interface ranged from -2.7 (uptake) to 19.9 mmol m^{-2} h^{-1} (emission) (1.4 [0.5, 3.1]; median [interquartile range (IQR)]; n = 107) and midnight fluxes ranged from -0.3 to 25.6 mmol m^{-2} h^{-1} (2.1 [0.9, 3.7]; n = 107) (Fig. 1a). Our measured fluxes are comparable to other studies conducted in temperate and boreal streams that used chambers [20,21] or empirical models [12,22,23], although they were in the lower range of the numbers modelled in a study in the USA [23] (Fig. S3). The lower numbers might be due to the lack of tributary inflows, large woody debris and strong hydraulic jumps in the selected stream sections (Supplementary Hand Out protocol).

To assess stream CO_2 flux variations between day and night, we computed the difference of night- minus day-time fluxes for each stream and sampling period, where positive numbers indicate an increase from day to night and vice versa (Fig. 1b). Differences in CO_2 fluxes amounted to 0.5 mmol m^{-2} h^{-1} [0.1, 1.4] (n = 107) across all sites and sampling periods, which is equivalent to a relative increase of 39% [4%, 100%] (n = 101; n reduced due to exclusion of relative comparisons to zero flux at day-time) (Fig. 2). Altogether, these results point towards a high relevance of night-time CO_2 fluxes as reported earlier for single pre-alpine streams[12], stream networks[13,17] or rivers[18]. A rough annual extrapolation of fluxes from our study sites (Supplementary Methods) shows that the inclusion of night-time fluxes increases annual estimates of site-specific stream CO_2 emissions by 16% [6%; 25%] (Table S4). Hence, our measurements and the simplified extrapolation of our data emphasize the need to collect and integrate night-time CO_2 flux data into sampling protocols as well as regional upscaling efforts.

Looking into the individual comparisons, we found 83 increases in median CO_2 fluxes from day to night with seven comparisons where the stream even switched from a sink to a source of CO_2 to the atmosphere (Table S3). However, we also found four comparisons where median CO_2 fluxes at day and night were the same and 20 decreases in the night (Table S3). These results and also other studies[13,24,25] suggest that the direction and strength of diel pCO_2 pattern can be largely variable across space and time.

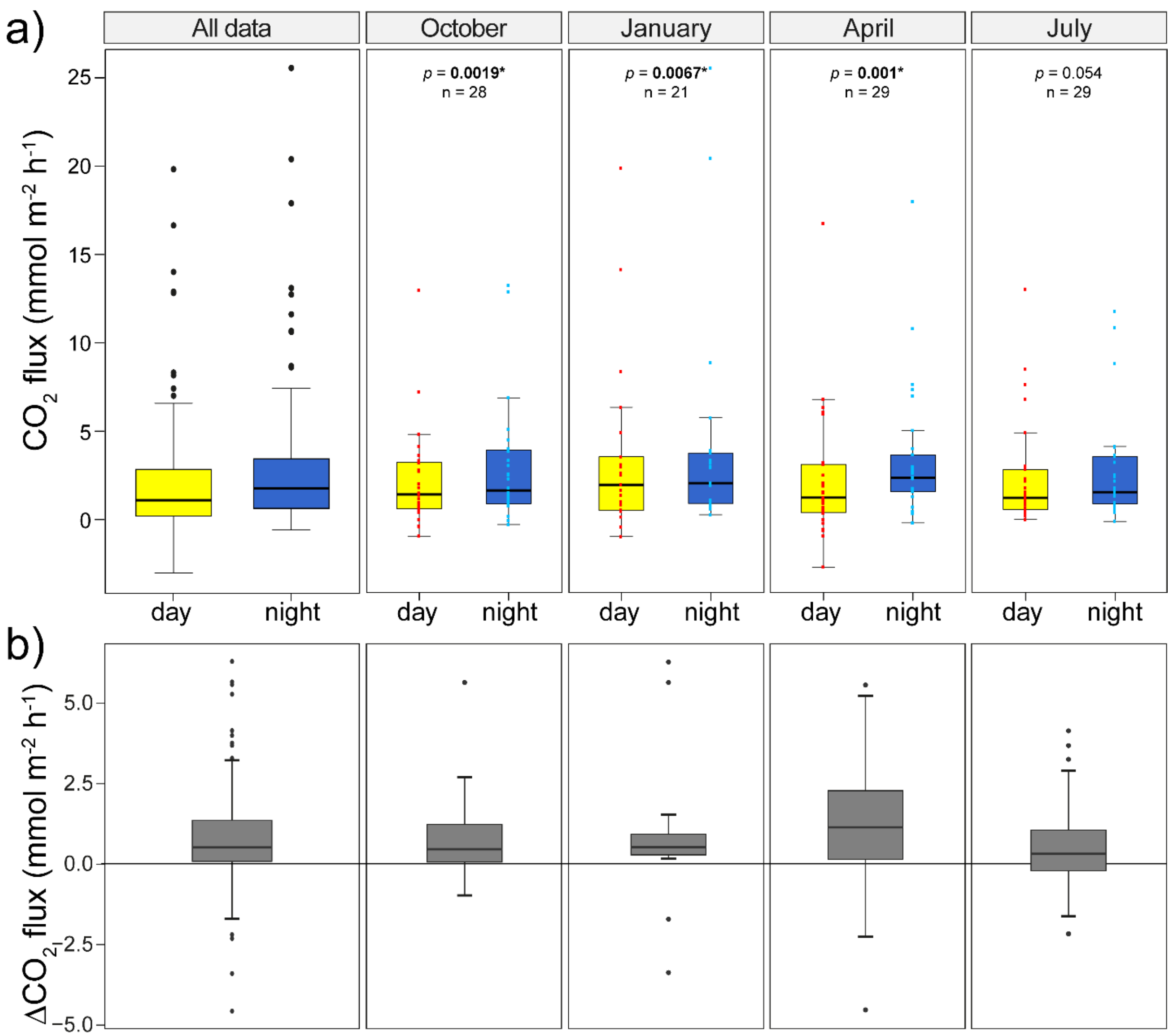

Figure 1. Day-to-night changes of CO_2 fluxes at the water-air interface of the sampled European streams. Stream CO_2 fluxes (in mmol CO_2 m^{-2} h^{-1}) at day- (yellow) and night-time (blue) (a) and the calculated changes from night minus day (ΔCO_2 flux) (b) for all data and separately for each sampling period. In the sampling periods comparisons in (a), CO_2 fluxes for individual stream sites are indicated by red (day) and light blue (night) dots. The boxplots visualize the median of all stream sites (line), the first and third quartiles (hinges), the 1.5 * inter-quartile ranges (whiskers), and the outliers outside the range of 1.5 * inter-quartile ranges (black dots). The differences in the CO_2 fluxes in mmol CO_2 m^{-2} h^{-1} from day to night are for October: 0.5 [0.1, 1.2]; January: 0.5 [0.3, 0.9]; April: 1.1 [0.1, 2.3]; July: 0.3 [-0.2, 1.1] (median [IQR]). On top of (a) are p values retrieved from paired comparisons of median CO_2 fluxes tested by Wilcoxon signed rank tests and the sample size (n). Significant p values with p <0.05 are in bold with an asterisk.

Diel CO_2 flux differences vary as a function of latitude and water temperature

The diel differences in CO_2 fluxes were significantly negatively related to latitude (Table 1A), with substantial diel variation more likely at lower latitudes. Likewise, the interaction with latitude and water temperature was significant (Table 1A), which might be explained by higher temperatures at lower latitudes during the sampling periods and higher solar radiation boosting in-stream primary production [26]. This dataset is derived from only 34 streams distributed across different climate zones in Europe. However, to our knowledge, it is currently the largest study of its kind, using flux chambers to measure CO_2 fluxes, and compare those fluxes at day- and night-time on such a spatial scale.

We found no significant differences in the magnitude of diel differences in CO_2 fluxes related to water temperature (Table 1A) using a linear mixed-effect model (LME). However, comparing the CO_2 fluxes at midday to midnight at the different sampling periods, we detected significant diel changes in CO_2 fluxes in October, January, and April (Fig. 1a). Contrary to our expectation that higher differences can be expected at higher temperatures, we did not detect significant changes from day to night in July (Fig. 1a), during which period the lowest changes in absolute numbers were recorded (0.3 mmol m^{-2} h^{-1}; Fig. 1b). The highest differences of CO_2 fluxes from day to night were measured during April (1.1 mmol m^{-2} h^{-1}), followed by January (0.5 mmol m^{-2} h^{-1}) and October (0.5 mmol m^{-2} h^{-1}). Lower day-night changes in July could be explained by increased riparian shading reducing photosynthesis [27,28]. For example, reduced in-stream photosynthesis in summer compared to spring has been shown for a subalpine stream network [28] or a temperate forested headwater stream [27]. However, comparing the canopy cover of the streams and the differences in CO_2 fluxes from day to night (Fig. S4h) revealed no clear pattern, whilst concurrent decreases from midday to midnight in oxygen and pH in July indicate higher ecosystem respiration, thus rejecting shade as a limiting factor (Fig. 3, Fig. S7c, f). A probable alternate explanation is that CO_2 production via photomineralization during the day counteracted a decrease via CO_2 fixation by photosynthesis[29] and diminished diel pCO_2 and ultimately CO_2 flux changes. This highlights the complex interplay between different light-dependent processes in streams influencing pCO_2 concentrations on a diel scale.

The importance of year-round measurement is highlighted by the January data set containing the second highest diel CO_2 flux changes. European ice-free streams may be perceived “dormant” during these periods and representative CO_2 flux estimates are thus often missing [3]. Our January data showed a magnitude of flux comparable to the rest of the year across the European streams as well as a high diel variability in CO_2 fluxes (Fig. 1). This may be attributed in part to the latitudinal coverage of our study as we included streams from the boreal to the Mediterranean. For example, the water temperatures of the Spanish streams were still relatively high in winter with around 2.8 - 9.5°C during the day whereas Swedish streams showed these temperatures in October and April. A study in the coterminous US looking into stream pCO_2 variability also reports varying strengths of diel pCO_2 variability, dependent on the investigated stream and time [24]. Hence, diel pCO_2 and CO_2 flux variability can be large in streams of the northern hemisphere, stressing the need to unravel the site-specific drivers of and mechanisms behind these diel changes.

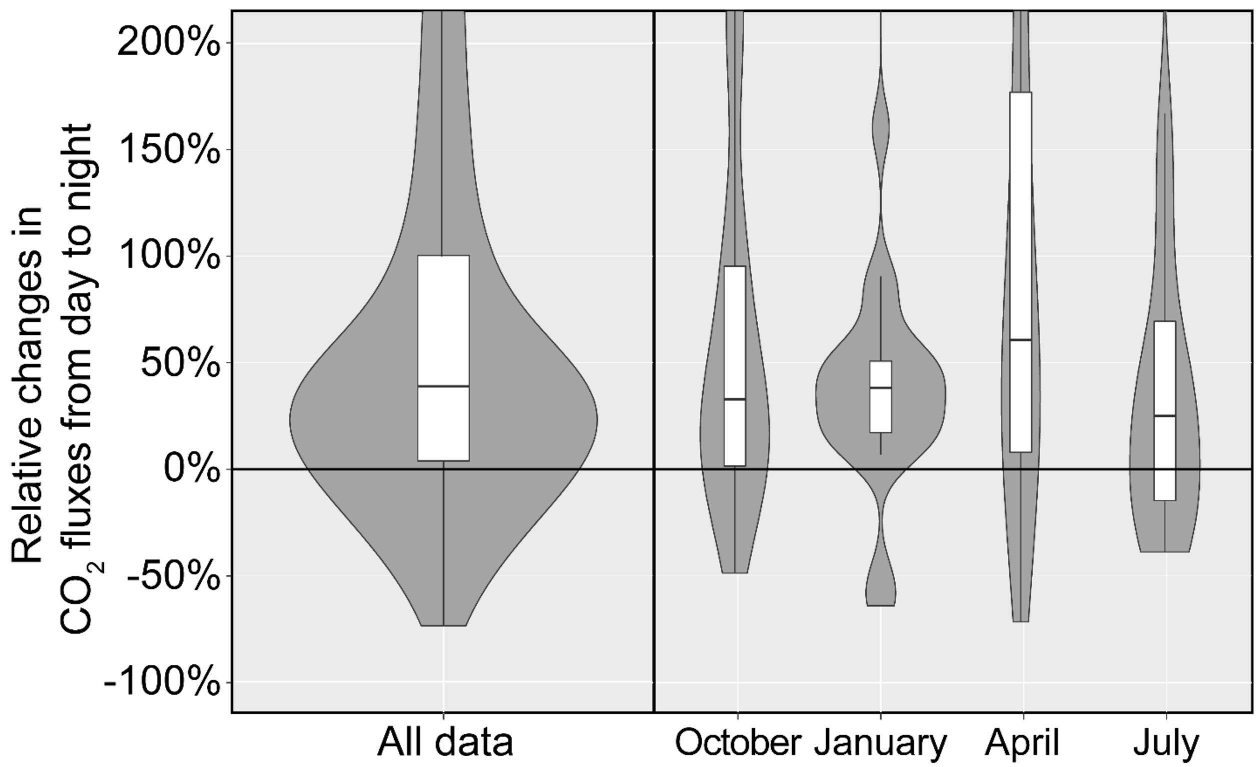

Figure 2. Relative changes in CO_2 fluxes from day to night (expressed as a %-change of the day-time values) for all data together and for each sampling period. A positive value indicates an increase in CO_2 fluxes during the night and vice versa. Outliers (> 1.5 * IQR) were excluded for illustration purposes as the large relative variation in these fluxes was due to minor absolute variation in fluxes close to zero. The median relative changes were positive throughout all sampling periods, ranging from 32% [0.6%, 95%] in October, 38% [16%, 50%] in January, 60% [7%, 177%] in April, to 24% [-16%, 69%] in July (median [IQR]; n = 26, 21, 28, and 26, respectively).

Diel CO_2 flux variability driven by changes in water pCO_2

To understand the mechanisms behind the observed changes in CO_2 fluxes from day to night, we first selected the two primary controls of CO_2 fluxes at the water-air interface, i.e., the gas exchange velocity and water pCO_2 and explored the influence of these parameters on absolute CO_2 flux changes using an LME. The diel CO_2 flux variability in European streams could be mostly attributed to changes in water pCO_2 (Table 1B), whereas changes in the gas exchange velocity k appeared less important. In fact, we did not measure significant variations in k from day to night in our streams (Fig. 3; Supplementary Fig. S5h).

In a second step, we tested the influence of biogeochemical parameters that vary on a diel scale on water pCO_2 day-to-night differences (Table 1C). This LME identified a link between the day-to-night changes in water pCO_2 and water dissolved O_2, with pCO_2 generally increasing and O_2 decreasing from day to night (Fig. S5b, c). This potentially reflects a diel cycle of CO_2 controlled by aquatic primary production and respiration (in-stream metabolism). Hence, even though *in situ* metabolism may play a minor role on determining the baseline pCO_2 and flux in smaller streams (mostly controlled by terrestrial inputs[23]), our results suggest that metabolism can be an important driver of the diel fluctuations in CO_2 fluxes. Indeed, increased water pCO_2 during the night has been attributed to a decrease in CO_2 fixation by primary producers [13,18], although a recent study suggests that the adjacent groundwater can also show measurable but less pronounced diel pCO_2 variations [30]. Previous research suggests that *in situ* mineralization of CO_2 should play a larger role in CO_2 dynamics in larger streams because they are less influenced by external

CO_2 sources [23]. Nevertheless, we did not find any trend in CO_2 flux day-to-night differences with stream width or discharge as a proxy for size (Fig. S4c, f) or with stream order (Fig. S6) although other studies suggest change over a size gradient [23,31]. Furthermore, the LME testing hydromorphological and catchment variables on pCO_2 day-to-night differences (Table 1D) did not reveal significant relationships with either of these drivers. This could either be due to the fact that we missed the best proxy that determines day-to-night differences in pCO_2 in European streams or that there are no common drivers among the investigated streams. A large diel variability of CO_2 patterns within one Swedish stream[32] or among US headwater streams[24] have been described, which complicates the identification of general drivers. Hence, further research is needed to decipher the diel variability of the sources and dynamics of pCO_2 in streams and to understand the environmental, hydromorphological, and catchment drivers before their importance on a regional or global scale can be assessed.

In-stream metabolism with photosynthetic CO_2 fixation diminishing pCO_2 during the day may explain the increase in CO_2 fluxes from day to night, but cannot explain why in some instances we measured a lower CO_2 flux at night. Potential explanations for a lower night flux might include: i) higher atmospheric CO_2 concentrations due to the absence of terrestrial CO_2 fixation during night and therefore a lower water-atmosphere pCO_2 gradient, ii) photomineralization of organic matter to CO_2 counteracting the CO_2 fixation by primary producers during day-time, and iii) lower turbulence due to a decrease in stream discharge in the night. We found significant increases in atmospheric CO_2 close to the investigated streams at night. However, this was usually accompanied by concomitant increases in water pCO_2 and therefore did not translate into smaller CO_2 gradients between the water-air interface (Fig. 3; Supplementary Fig. S4b, e, i). A production of CO_2 due to photomineralization of dissolved organic carbon (DOC) could play a role in diel CO_2 dynamics in streams with high amounts of colored terrestrial organic matter[33]. In the highly-colored streams, diel CO_2 patterns can additionally be influenced by DOC shading diminishing benthic primary production[34]. In October, we measured DOC concentrations in a subset of the investigated streams for another study[35] where an agricultural stream in Sweden and peatland-dominated streams in Great Britain had high DOC concentrations (>10 mg L^{-1}) whereas the median DOC was much lower with 2.6 mg L^{-1} [35]. Due to the limited data, we could not test the effect of DOC on pCO_2 changes and we can neither confirm nor exclude that photomineralization might play a role for diel pCO_2 and consequently CO_2 flux variability in the studied streams. We did find, nonetheless, that the majority of the streams where CO_2 fluxes were lower during the night also had a lower gas transfer velocity (k_{600}), likely due to a slight decrease in stream discharge and therefore turbulence. Thus, while there was a general tendency of increased pCO_2 from day to night (only four out of 20 decreases in CO_2 fluxes from day to night showed a concomitant decrease in water pCO_2), individual streams at single time points seemed to experience diel fluctuations in discharge as described elsewhere[36]. This can simultaneously reduce the gas exchange velocity of the stream and therefore cause lower night-time CO_2 fluxes. In this study we only measured stream discharge during the day, and therefore the importance of this mechanism remains to be confirmed.

Table 1. Results of the linear mixed-effect models (LME). The effects of latitude and water temperature during the day (A) and the effect of day-to-night differences of pCO_2 and the gas transfer velocity (Δ = night minus day values) (B) on the day-to-night difference of CO_2 fluxes were tested. Furthermore, the effect of day-to-night differences of physical and biogeochemical parameters (C) and the effect of catchment and hydromorphological related parameters (D) on the day-to-night differences of pCO_2 were evaluated. Stream ID was included as a random effect on the intercept. Significances of fixed effects were assessed with likelihood ratio tests with degrees of freedom = 1. The slope direction (sign) of the effect is indicated with – or + when significant. Significant *p* values <0.05 are in bold.

Response variable	**Fixed effect**	**χ^2 (1)**	***p***	**sign**
A) Testing spatial and temporal hypotheses				
CO_2 flux difference from day to night	latitude	7.4207	**0.006**	**-**
	water temperature (day)	0.0168	0.897	
	water temperature (day) * latitude	4.9594	**0.026**	+
B) Testing physical and biogeochemical drivers of CO_2 flux changes				
CO_2 flux difference from day to night	Δ water pCO_2	4.9497	**0.026**	**+**
	Δ gas transfer velocity *k*	0.5613	0.454	
C) Testing biogeochemical drivers of pCO_2 changes				
pCO_2 difference from day to night	Δ water O_2 concentration	7.9879	**0.005**	**-**
	Δ pH	0.0345	0.853	
	Δ conductivity	0.0293	0.864	
	Δ Tw-Ta* (proxy for heat flux)	1.6720	0.196	
	Δ water temperature	0.8731	0.350	
D) Testing catchment and hydromorphological drivers of pCO_2 changes				
pCO_2 difference from day to night	day length	1.7244	0.189	
	stream wetted width	0.3748	0.540	
	discharge	3.4458	0.063	
	%forest	0.0950	0.758	
	catchment area	2.3656	0.124	

* Heat flux calculated as water temperature (Tw) minus air temperature (Ta).
A) Marginal R^2 = 0.12, conditional R^2 = 0.18, sample size =107.
B) Marginal R^2 = 0.08, conditional R^2 = 0.10, sample size = 77.
C) Marginal R^2 = 0.13, conditional R^2 = 0.33, sample size = 78.
D) Marginal R^2 = 0.11, conditional R^2 = 0.13, sample size = 68.

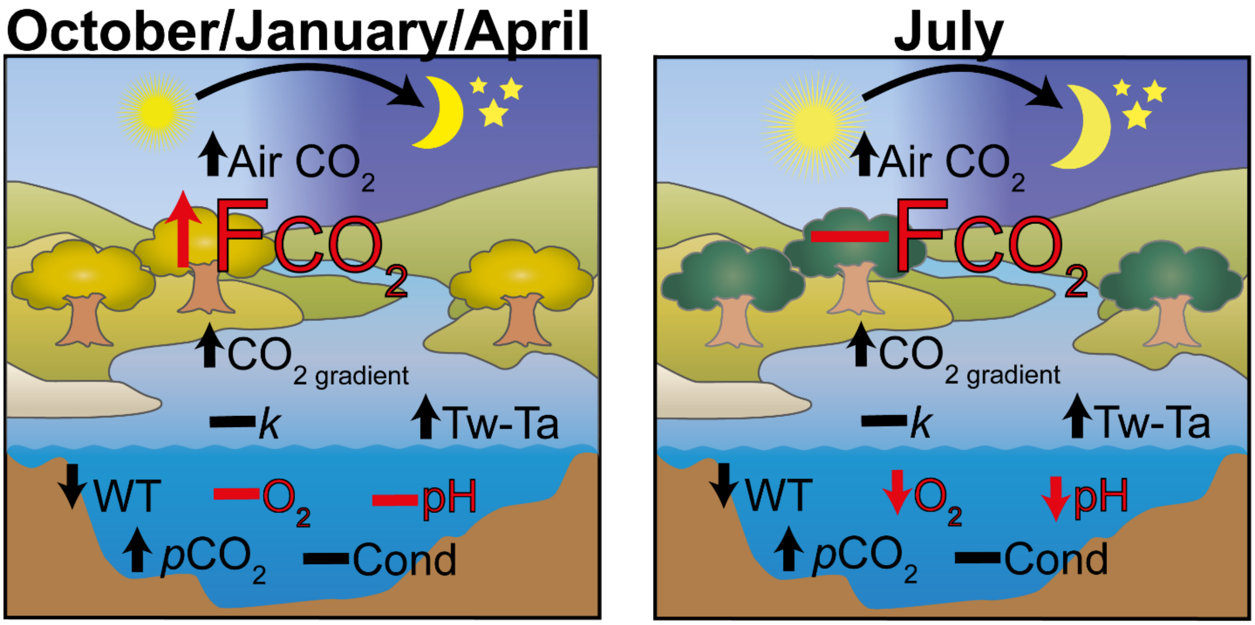

Figure 3. Diel changes in CO_2 fluxes (F_{CO_2}) and other physical and chemical parameters for October/January/April and July, respectively. The physical and chemical parameters comprise atmospheric CO_2 (Air CO_2), the differences of CO_2 concentrations in the water minus the air ($CO_{2\ gradient}$), the water-air gas transfer velocity (k), the differences of temperatures in the water minus the air (Tw-Ta), the water temperature (WT), the oxygen concentration in the water (O_2), pH in the water, the partial pressure of CO_2 in the water (pCO_2), and conductivity (Cond). The arrows indicate significant increases (↑) or significant decreases (↓) from day to night and the line indicates no significant change (—) tested by a Wilcoxon signed rank test (see Supplementary Fig. S5 for more information). The differences between the sampling periods October/January/April (left) and July (right) detected in this European study are highlighted in red.

Maximum CO_2 flux differences might be even higher - limitations of the study design

For organizational reasons, the sampling scheme of this collaborative study was standardized to fixed times of measurements for the day and the night. All teams across Europe started their measurements at 11:00 (midday) and 23:00 GMT (midnight) during each sampling period, which has consequences for the magnitude of the observed diel variability of the CO_2 fluxes. Largest diel differences in stream pCO_2 concentrations have generally been detected at the end of the day compared to the end of the night [12,18,37]. In an agricultural Swedish stream, diel maximum and minimum CO_2 concentrations were reached at 04:00 and 16:00 (GMT), respectively, during spring and early summer periods (late April to early July) where diel dynamics were most pronounced[25]. In these scenarios, sampling midday and midnight, as conducted in this study, would be close to those maxima and minima as they can be reached already earlier during the day (see Fig. S7 in May). However, the maxima and minima of diel CO_2 dynamics in streams can vary largely (see Fig. S7 in October, April, July). In another example of German streams[37], the times of minima and maxima differ between streams and times, and the fixed time points chosen in this study would miss the maximum differences that can be observed (see Fig. S8 in August). Hence, our estimates could be conservative as we compared fixed time points at midday and midnight. In general, CO_2 flux measurements in streams are highly sensitive towards the time of the day because diel minimum and maximum of pCO_2 can vary largely from month to month but also from day to day. As we found that the diel variability of pCO_2 was the major driver of diel CO_2 fluxes, we recommend future studies that plan to measure CO_2 fluxes directly with the chamber method, to additionally monitor the diel variability of pCO_2 with loggers at a high resolution. This approach will provide the opportunity to estimate if the measurements are done during peak times or not.

While our results provide a first insight into the drivers of day-night differences in CO_2 fluxes, the high uncertainty in the models as well as the sometimes opposing patterns - increases and decreases from day to night in different streams and sampling periods - point towards different drivers varying on a temporal and spatial scale. We recommend that future study designs incorporate high-frequency CO_2 data together with biogeochemical variables from the stream (e.g., O_2) and the atmosphere (e.g., CO_2 or temperature) [38]. Additionally, we recommend including radioactive or stable carbon isotope signatures to track potential sources of CO_2 and their changes in streams [39,40] to better assess terrestrial-aquatic linkages. Linking temporal patterns of fluvial CO_2 fluxes with its drivers across large spatial scales is a path towards a more accurate understanding of their role in regional and global carbon cycles. Our results demonstrate that, in many streams across Europe, night-time CO_2 fluxes exceed day-time, resulting in a potential underestimation of global CO_2 emissions from inland waters if not considered. It is thus critical to account for the diel variability of fluvial CO_2 fluxes for accurate daily and annual estimates of CO_2 emissions from inland waters.

Methods

Sampling scheme

The project included 16 teams distributed across 11 European countries. Every team sampled one to three streams every three months (October 2016/January 2017/April 2017/July 2017) within a time frame of two weeks throughout a whole year. These sampling periods roughly cover the seasons autumn/winter/spring/summer although, due to the large latitudinal coverage of the sampling sites, the seasons and their characteristics vary largely. In total, 34 stream sites (Fig. S1) were visited each sampling period during the specified two weeks' time frame except for 11 streams in January that were frozen during the sampling weeks (Table S3).

CO_2 fluxes were measured once every sampling period with drifting flux chambers equipped with CO_2 sensors. This method has proven to be a reliable and least biased direct measurement of CO_2 fluxes at the water-air interface in streams [19,41]. CO_2 concentrations in the chamber headspace were logged every 30 seconds over a period of 5 to 10 minutes during each run, and CO_2 fluxes were calculated based on the rate of change over time in pCO_2 in the chamber headspace. At each stream, we measured CO_2 fluxes with the flux chamber (five times), pCO_2 concentration in the atmosphere and water with the CO_2 sensors in the flux chamber (details described in Supplementary Methods), pH, temperature, conductivity, and oxygen in the water with a multiprobe (Table S2). These measurements were started at 11:00 and 23:00 (GMT) and lasted approximately two hours and are referred to as midday and midnight throughout this article. Stream width, depth, canopy cover, and discharge were determined during the day (see Supplementary Hand Out protocol for details). In addition, the following information were collected for each stream once during the study: stream order, climate zone, catchment area until the endpoint of the investigated stream site and the percentage of coverage of different land use classes in this catchment area, and predominant geology (Table S1).

Calculations of CO_2 fluxes and gas transfer velocity

Flux rates were obtained from the linear slopes of the pCO_2 in the chamber headspace over time and a flux was accepted if the coefficient of determination (R^2) of the slope was at least 0.65 [42]. An exception was made in cases where the slope was close to zero and the pCO_2 concentrations in the atmosphere and water (measured at the same time) were at equilibrium. These fluxes were set to zero. Final flux rates F (mmol CO_2 m^{-2} h^{-1}) were calculated according to Eq. (1) [43]:

$$F = S * 10^{-3} \frac{PV}{RTA} * 60 * 60, \tag{1}$$

where S is the slope (ppm s^{-1}), P is the pCO_2 concentration in the atmosphere (atm), V is the volume (mL) of the drifting chamber, R is the gas constant (82.0562 mL atm K^{-1} mol^{-1}), T is the chamber air temperature (K), A is the bottom area of the chamber (m^2), and the last term is the conversion from seconds to hours. In this study, we followed the sign convention whereby positive values indicate a CO_2 flux from the stream to the atmosphere (source) and negative values indicate a flux from the atmosphere to the stream (sink). The magnitudes of variations between day- and night-time measurements are additionally stated as percent increases, which were computed by dividing the difference between the values at night minus day by the value at day and expressing the result as a percent change from day to night.

We used F (Eq. 1) to calculate the gas transfer velocity (k in cm h^{-1}) by inverting the equation for Fick's law of gas diffusion, according to Eq. (2):

$$k = \frac{F}{kH\left(CO_{2_{water}} - CO_{2_{air}}\right)} * 100, \tag{2}$$

where kH is Henry's constant (in mol L^{-1} atm^{-1}) adjusted for temperature [44].

For comparison of transfer velocities between sites and sampling periods and with the literature, k (Eq. 2) was standardized to k_{600} (Eq. 3):

$$k_{600} = k\left(\frac{600}{S_c}\right)^{-0.5}, \tag{3}$$

where k is the transfer velocity at *in situ* temperature (T), Sc is the Schmidt number for *in situ* temperature T, the Schmidt number for 20°C in freshwater is 600, and representing a hydrodynamic rough water surface typical in streams the exponent of -0.5 was chosen [45].

Statistical analyses

All statistical analyses were performed with median values of three to five floating chamber runs per day and night, respectively, using the statistical programming language R [46] (version 3.5.1). Samplings that generated less than three values for either day or night due to an R^2 of the slope < 0.65 [42] were excluded from further analysis reducing the number from 136 to 107 day-night comparisons. For our statistical tests, the alpha level was set to $\alpha = 0.05$. Significant differences between day- and night-time measurements for each sampling period across all streams were tested with Wilcoxon signed rank tests [47] where median day- and night-time values for each stream site were paired (Fig. 1a). The same tests were conducted for the other biogeochemical variables measured at midday and midnight (see Fig. 3; Fig. S5).

With a first linear mixed-effect model (LME) we tested the latitudinal and water temperature effect on CO_2 flux differences from day to night. A second LME was built to evaluate the two major drivers of CO_2 flux differences from day to night: pCO_2 and gas exchange velocity (k). A third LME was subsequently used to determine the biochemical factors potentially influencing the differences of night- minus day-time pCO_2, which was identified as the only significant driver in the second LME. Finally, a fourth LMW was built to evaluate the effect of catchment and hydromorphological parameters on the day-to-night differences of pCO_2. For these tests, we used the “lmer” function of the R-package “lme4” [48] with Maximum Likelihood estimation. Fixed effects for the LME with biogeochemical parameters for pCO_2 differences from day to night included absolute differences from day to night of oxygen concentration in the water, pH, conductivity, temperature gradient of atmosphere and water, and water temperature. Fixed effects for the LME with catchment and hydromorphological parameters included day length (i.e., sun hours from sunrise to sunset), stream wetted width, discharge, % forest of the catchment, and catchment area. These variables are mostly remotely available for streams. For the LMEs we included stream ID as a random effect allowing different intercepts for each stream to account for pseudoreplication (one data point per sampling period per stream) and z-scaled all fixed effects with the “scale” function before running the models. Statistical significances of fixed effects were assessed with likelihood ratio tests using the function “drop1” [49]. The respective LMEs were followed by a model validation, checking the residuals for normal distribution and homogeneity of variances[50]. A separation of the dataset to check if drivers between increases from day to night and decreases from day to night differ, did not reveal acceptable models in terms of model validation (i.e., residuals were not normally distributed). Although our dataset provided a large spatial coverage on day-night differences in CO_2 fluxes in European streams, it did not have the statistical power to test for significant drivers separately for increases and decreases.

Data Availability

The data that support the findings of this study are openly available in figshare at http://doi.org/10.6084/m9.figshare.12717188.

Code Availability

This manuscript includes no code.

References

1. Butman, D. E. *et al.* Aquatic carbon cycling in the conterminous United States and implications for terrestrial carbon accounting. *Proc. Natl. Acad. Sci.* **113**, 58–63 (2016).

2. Drake, T. W., Raymond, P. A. & Spencer, R. G. M. Terrestrial carbon inputs to inland waters: A current synthesis of estimates and uncertainty. *Limnol. Oceanogr. Lett.* **3**, 132–142 (2018).

3. Raymond, P. A. *et al.* Global carbon dioxide emissions from inland waters. *Nature* **503**, 355–359 (2013).

4. MacIntyre, S., Wanninkhof, R. & Chanton, J. P. Trace gas exchange in freshwater and coastal marine systems: flux across the air water interface. in *Methods in Ecology: Biogenic Trace Gases: Measuring Emissions from Soil and Water* 52–97 (Blackwell Publishing, 1995).

5. Duvert, C., Butman, D. E., Marx, A., Ribolzi, O. & Hutley, L. B. CO2 evasion along streams driven by groundwater inputs and geomorphic controls. *Nat. Geosci.* **11**, 813–818 (2018).

6. Rocher-Ros, G., Sponseller, R. A., Lidberg, W., Mörth, C. & Giesler, R. Landscape process

domains drive patterns of CO2 evasion from river networks. *Limnol. Oceanogr. Lett.* **4**, 87–95 (2019).

7. Hall, R. O. & Ulseth, A. J. Gas Exchange in Streams and Rivers. *WIREs Water* e1391 (2019). doi:10.1002/wat2.1391

8. Hope, D., Palmer, S. M., Billet, M. F. & Dawson, J. J. C. Variations in dissolved CO2 and CH4 in a first-order stream and catchment: an investigation of soil-stream linkages. *Hydrol. Process.* **18**, 3255–3275 (2004).

9. Horgby, Å., Gómez-Gener, L., Escoffier, N. & Battin, T. J. Dynamics and potential drivers of CO2 concentration and evasion across temporal scales in high-alpine streams. *Environ. Res. Lett.* **14**, 124082 (2019).

10. Guasch, H., Armengol, J., Martí, E. & Sabater, S. Diurnal variation in dissolved oxygen and carbon dioxide in two low-order streams. *Water Res.* **32**, 1067–1074 (1998).

11. Lynch, J. K., Beatty, C. M., Seidel, M. P., Jungst, L. J. & DeGrandpre, M. D. Controls of riverine CO2 over an annual cycle determined using direct, high temporal resolution pCO2 measurements. *J. Geophys. Res.* **115**, G03016 (2010).

12. Peter, H. *et al.* Scales and drivers of temporal pCO2 dynamics in an Alpine stream. *J. Geophys. Res. Biogeosciences* **119**, 1078–1091 (2014).

13. Rocher-Ros, G., Sponseller, R. A., Bergstr, A.-K., Myrstener, M. & Giesler, R. Stream metabolism controls diel patterns and evasion of CO2 in Arctic streams. *Glob. Chang. Biol.* **00**, 1–14 (2019).

14. Koehler, B., Landelius, T., Weyhenmeyer, G. A., Machida, N. & Tranvik, L. J. Sunlight-induced carbon dioxide emissions from inland waters. *Global Biogeochem. Cycles* **28**, 696–711 (2014).

15. Golub, M., Desai, A. R., McKinley, G. A., Remucal, C. K. & Stanley, E. H. Large Uncertainty in Estimating pCO2 From Carbonate Equilibria in Lakes. *J. Geophys. Res. Biogeosciences* **122**, 2909–2924 (2017).

16. Raymond, P. A. *et al.* Scaling the gas transfer velocity and hydraulic geometry in streams and small rivers. *Limnol. Oceanogr. Fluids Environ.* **2**, 41–53 (2012).

17. Schelker, J., Singer, G. A., Ulseth, A. J., Hengsberger, S. & Battin, T. J. CO2 evasion from a steep, high gradient stream network: importance of seasonal and diurnal variation in aquatic pCO2 and gas transfer. *Limnol. Oceanogr.* **61**, 1826–1838 (2016).

18. Reiman, J. H. & Xu, Y. J. Diel variability of pCO2 and CO2 outgassing from the lower Mississippi River: Implications for riverine CO2 outgassing estimation. *Water* **11**, 43 (2019).

19. Bastviken, D., Sundgren, I., Natchimuthu, S., Reyier, H. & Gålfalk, M. Technical Note: Cost-efficient approaches to measure carbon dioxide (CO2) fluxes and concentrations in terrestrial and aquatic environments using mini loggers. *Biogeosciences* **12**, 3849–3859 (2015).

20. Looman, A., Maher, D. T., Pendall, E., Bass, A. & Santos, I. R. The carbon dioxide evasion cycle of an intermittent first-order stream: contrasting water–air and soil–air exchange. *Biogeochemistry* **132**, 87–102 (2017).

21. Crawford, J. T. *et al.* CO2 and CH4 emission from streams: Patterns, controls, and regional significance. *Global Biogeochem. Cycles* **28**, 197–210 (2014).

22. Teodoru, C. R., Del Giorgio, P. A., Prairie, Y. T. & Camire, M. Patterns in pCO2 in boreal streams

and rivers of northern Quebec, Canada. *Global Biogeochem. Cycles* **23**, GB2012 (2009).

23. Hotchkiss, E. R. *et al.* Sources of and processes controlling CO2 emissions change with the size of streams and rivers. *Nat. Geosci.* **8**, 696–699 (2015).

24. Crawford, J. T., Stanley, E. H., Dornblaser, M. M. & Striegl, R. G. CO2 time series patterns in contrasting headwater streams of North America. *Aquat. Sci.* **79**, 473–486 (2016).

25. Wallin, M. B., Audet, J., Peacock, M., Sahlée, E. & Winterdahl, M. Carbon dioxide dynamics in an agricultural headwater stream driven by hydrology and primary production. *Biogeosciences* **17**, 2487–2498 (2020).

26. Demars, B. O. L. *et al.* Impact of warming on CO2 emissions from streams countered by aquatic photosynthesis. *Nat. Geosci.* **9**, 758–761 (2016).

27. Roberts, B. J., Mulholland, P. J. & Hill, W. R. Multiple scales of temporal variability in ecosystem metabolism rates: Results from 2 years of continuous monitoring in a forested headwater stream. *Ecosystems* **10**, 588–606 (2007).

28. Ulseth, A. J., Bertuzzo, E., Singer, G. A., Schelker, J. & Battin, T. J. Climate-Induced Changes in Spring Snowmelt Impact Ecosystem Metabolism and Carbon Fluxes in an Alpine Stream Network. *Ecosystems* **21**, 373–390 (2018).

29. Cory, R. M., Ward, C. P., Crump, B. C. & Kling, G. W. Sunlight controls water column processing of carbon in arctic fresh waters. *Science.* **345**, 925–928 (2014).

30. Riml, J., Campeau, A., Bishop, K. & Wallin, M. B. Spectral Decomposition Reveals New Perspectives on CO2 Concentration Patterns and Soil-Stream Linkages. *J. Geophys. Res. Biogeosciences* **124**, 3039–3056 (2019).

31. Liu, S. & Raymond, P. A. Hydrologic controls on pCO2 and CO2 efflux in US streams and rivers. *Limnol. Oceanogr. Lett.* **3**, 428–435 (2018).

32. Wallin, M. B., Audet, J., Peacock, M., Sahlée, E. & Winterdahl, M. Carbon dioxide dynamics in an agricultural headwater stream driven by hydrology and primary production. *Biogeosciences* **17**, 2487–2498 (2020).

33. Lindell, M. J., Granéli, H. W. & Bertilsson, S. Seasonal photoreactivity of dissolved organic matter from lakes with contrasting humic content. *Can. J. Fish. Aquat. Sci.* **57**, 875–885 (2000).

34. Ask, J., Karlsson, J., Persson, L. & Ask, P. Terrestrial organic matter and light penetration: Effects on bacterial and primary production in lakes. *Limnol. Oceanogr.* **54**, 2034–2040 (2009).

35. Bravo, A. G. *et al.* The interplay between total mercury, methylmercury and dissolved organic matter in fluvial systems: A latitudinal study across Europe. *Water Res.* **144**, (2018).

36. Schwab, M., Klaus, J., Pfister, L. & Weiler, M. Diel discharge cycles explained through viscosity fluctuations in riparian inflow. *Water Resour. Res.* **52**, 8744–8755 (2016).

37. Bodmer, P., Heinz, M., Pusch, M., Singer, G. & Premke, K. Carbon dynamics and their link to dissolved organic matter quality across contrasting stream ecosystems. *Sci. Total Environ.* **553**, 574–586 (2016).

38. Vachon, D. *et al.* Paired O2-CO2 measurements provide emergent insights into aquatic ecosystem function. *Limnol. Oceanogr. Lett.* (2019).

39. Campeau, A. *et al.* Stable Carbon Isotopes Reveal Soil-Stream DIC Linkages in Contrasting

Headwater Catchments. *J. Geophys. Res. Biogeosciences* **123**, 149–167 (2018).

40. Campeau, A. *et al.* Current forest carbon fixation fuels stream CO2 emissions. *Nat. Commun.* **10**, 1–9 (2019).

41. Lorke, A. *et al.* Technical note: Drifting versus anchored flux chambers for measuring greenhouse gas emissions from running waters. *Biogeosciences* **12**, 7013–7024 (2015).

42. Tremblay, A., Varfalvy, L., Garneau, M. & Roehm, C. *Greenhouse gas Emissions-Fluxes and Processes: hydroelectric reservoirs and natural environments*. (Springer Science & Business Media, 2005).

43. Duc, N. T. *et al.* Automated Flux Chamber for Investigating Gas Flux at Water–Air Interfaces. *Environ. Sci. Technol.* **47**, 968–975 (2013).

44. Goldenfum, J. A. *GHG Measurement Guidelines for Freshwater Reservoirs: Derived From: The UNESCO/IHA Greenhouse Gas Emissions from Freshwater Reservoirs Research Project*. (International Hydropower Association (IHA), 2010).

45. Jähne, B. *et al.* On the parameters influencing air-water gas exchange. *J. Geophys. Res. Ocean.* **92**, 1937–1949 (1987).

46. R Core Team. R: A language and environment for statistical computing. *R Found. Stat. Comput. Vienna, Austria* (2018).

47. Wilcoxon, F. Individual Comparisons by Ranking Methods. *Biometrics Bull.* **1**, 80–83 (1945).

48. Bates, D., Maechler, M., Bolker, B. & Walker, S. Fitting Linear Mixed-Effects Models Using lme4. *J. Stat. Softw.* **67**, 1–48 (2015).

49. Zuur, A., Ieno, E. N., Walker, N., Saveliev, A. A. & Smith, G. M. *Mixed effects models and extensions in ecology with R*. (Springer Science & Business Media, 2009).

50. Zuur, A. F. & Ieno, E. N. A protocol for conducting and presenting results of regression-type analyses. *Methods Ecol. Evol.* **7**, 636–645 (2016).

Acknowledgements

We thank the initiators of the first Collaborative European Freshwater Science Project for Young Researchers, the European Federation of Freshwater Sciences (EFFS) board, the European Fresh and Young Researchers (EFYR) and the representatives of the Fresh Blood for Fresh Water (FBFW) meetings. We also thank the seven national freshwater societies financing this project, namely the Iberian Association of Limnology (AIL; Spain and Portugal), Deutsche Gesellschaft für Limnologie e.V. (DGL; Germany), Swiss Society for Hydrology and Limnology (SGHL; Switzerland), Italian Association of Oceanography and Limnology (Italy), Freshwater Biological Association (FBA; United Kingdom), French Limnological Association (AFL; France), Austrian Limnological Society (SIL-Austria), as well as the Leibniz-Institute of Freshwater Ecology and Inland Fisheries for additional funds. Additional funding was awarded to J.P.C.-R. by a Juan de la Cierva postdoctoral grant from the Spanish Government (FJC2018-037791-I), to A.P.P. by a PhD grant from the Fundação para a Ciência e Tecnologia (SFRH/BD/115030/2016), to B.C.D. by the Marine Institute's Cullen PhD fellowship (Grant No. CF/15/05), to N.C. by the European Union's Horizon 2020 research and innovation programme under the Marie Sklodowska-Curie grant agreement (No.839709), to J.M. by FCT (Portuguese Science Foundation) through a PhD grant (SFRH/BD/131924/2017), to J.P. by the DSI/NRF Research Chair in Inland

Fisheries and Freshwater Ecology, to A.F. by the Juan de la Cierva postdoctoral grant from the Spanish Government (FJCI-2017–33171), to C. M-L. by the French National Agency for Water and Aquatic Environments (ONEMA, Action 13, “Colmatage, échanges nappe-rivière et processus biogéochimiques”). We acknowledge Luigi Naselli-Flores and Antonio Camacho for their encouragement and support during the project. We also thank David Bastviken, Ingrid Sundgren, and Thanh Duc Nguyen for the introduction to the logger and chamber construction and advice for measurements of CO_2 fluxes with the chamber and Vincent Fugère for his help in setting up the linear mixed-effect models. Furthermore, we are very thankful to Rafael Marcé and Paul del Giorgio for their thoughtful comments on the manuscript. Finally, we thank three anonymous reviewers for constructive inputs that improved the manuscript.

Author contributions

K.A. and P.B. conceived the study design, coordinated the project and contributed equally to this work; all authors collected and analyzed the field data and K.A. and P.B. gathered and performed the quality check of all data; K.A., P.B. and J.P.C.-R. co-wrote the paper with the help of M.K., G.H.N., and N.C. All authors commented on the manuscript.

Competing interest statement

The authors declare no competing interests.

Supplementary Methods and Results

Carbon dioxide fluxes increase from day to night across European streams

Katrin Attermeyer[1,2,3], Joan Pere Casas-Ruiz[4,5], Thomas Fuss[6], Ada Pastor[4,5,7], Sophie Cauvy-Fraunié[8], Danny Sheath[9,10], Anna C. Nydahl[1], Alberto Doretto[11,12], Ana Paula Portela[13,14], Brian C. Doyle[15], Nikolay Simov[16], Catherine Gutmann Roberts[9], Georg H. Niedrist[17], Xisca Timoner[4,5], Vesela Evtimova[18], Laura Barral-Fraga[5], Tea Bašić[9,19], Joachim Audet[20,21], Anne Deininger[22,23], Georgina Busst[9], Stefano Fenoglio[12,24], Núria Catalán[4,5,25], Elvira de Eyto[26], Francesca Pilotto[22,27], Jordi-René Mor[4,28], Juliana Monteiro[29], David Fletcher[9], Christian Noss[30], Miriam Colls[4,5], Magdalena Nagler[31], Liu Liu[30,32], Clara Romero González-Quijano[33], Ferran Romero[4,5], Nina Pansch[32], José L. J. Ledesma[20,34,35], Josephine Pegg[9,36], Marcus Klaus[22,37], Anna Freixa[4,5], Sonia Herrero Ortega[32], Clara Mendoza-Lera[8,30], Adam Bednařík[38,39], Jérémy A. Fonvielle[32], Peter J. Gilbert[40], Lyubomir A. Kenderov[41], Martin Rulík[38], Pascal Bodmer[30,42,43]*

1 Limnology/Department of Ecology and Genetics, Uppsala University, 75236 Uppsala, Sweden

2 WasserCluster Lunz – Biologische Station, 3293 Lunz am See, Austria

3 Department of Functional and Evolutionary Ecology, University of Vienna, 1090 Vienna, Austria

4 Catalan Institute for Water Research (ICRA), 17003 Girona, Spain

5 Department of Environmental Sciences, University of Girona (UdG), 17003 Girona, Spain

6 Fluvial Ecosystem Ecology, Department of Ecology, University of Innsbruck, 6020 Innsbruck, Austria

7 present address: Department of Biology, Aarhus University, 8000 Aarhus C, Denmark

8 INRAE, UR Riverly, Centre de Lyon-Villeurbanne, Villeurbanne Cedex, France

9 Department of Life and Environmental Sciences, Bournemouth University, BH12 5BB, UK

10 present address: Institute of Global Health, Faculty of Medicine, University of Geneva, Campus Biotech, 1211 Geneva, Switzerland

11 Department of Sciences and Technological Innovation, University of Piemonte Orientale, 15121 Alessandria, Italy

12 ALPSTREAM – Alpine Stream Research Center, 12030 Ostana, Italy

13 Research Centre in Biodiversity and Genetic Resources (CIBIO-InBIO), University of Porto, 4485-661 Vila do Conde, Portugal

14 Faculty of Sciences, University of Porto, 4169-007 Porto, Portugal

15 Centre for Freshwater and Environmental Studies, Dundalk Institute of Technology, Dundalk, Co Louth, A91 K584, Ireland

16 National Museum of Natural History, Bulgarian Academy of Sciences, 1000 Sofia, Bulgaria

17 River and Conservation Research, Department of Ecology, University of Innsbruck, 6020 Innsbruck, Austria

18 Department of Aquatic Ecosystems, Institute of Biodiversity and Ecosystem Research, Bulgarian Academy of Sciences, 1000 Sofia, Bulgaria

19 present address: Centre for Environment, Fisheries and Aquaculture Science (Cefas), Pakefield Road, Lowestoft, Suffolk NR33 OHT, UK

20 Department of Aquatic Sciences and Assessment, Swedish University of Agricultural Sciences, 75007 Uppsala, Sweden

21 present address: Department of Bioscience, Aarhus University, 8600 Silkeborg, Denmark

22 Department of Ecology and Environmental Science, Umeå University, 90736 Umeå, Sweden

23 present address: Norwegian Institute for Water Research, 0349 Oslo, Norway

24 Department of Life Sciences and Systems Biology, University of Turin, 10124 Turin, Italy

25 present address: Laboratoire des Sciences du Climat et de l'Environnement (LSCE), CEA, CNRS, UVSQ, 91191 Gif-Sur-Yvette, France / United States Geological Survey, Boulder, CO 80303, USA

26 Marine Institute, Furnace, Newport, Co Mayo F28 PF65, Ireland

27 present address: Environmental Archaeology Lab, Department of Historical, Philosophical and Religious studies, Umeå University, 90736 Umeå, Sweden

28 Department of Evolutionary Biology, Ecology and Environmental Sciences, Faculty of Biology, University of Barcelona (UB), 08028 Barcelona, Spain

29 Centre for Ecology, Evolution and Environmental Changes (cE3c), Faculdade de Ciências, Universidade de Lisboa, 1749-016 Lisboa, Portugal

30 Institute for Environmental Sciences, University of Koblenz-Landau, 76829 Landau, Germany

31 Institute of Microbiology, University of Innsbruck, 6020 Innsbruck, Austria

32 Experimental Limnology, Leibniz-Institute of Freshwater Ecology and Inland Fisheries (IGB), 16775 Stechlin, Germany

33 Ecohydrology, Leibniz-Institute of Freshwater Ecology and Inland Fisheries (IGB), 12587 Berlin, Germany

34 Center for Advanced Studies of Blanes, Spanish National Research Council, 17300 Blanes, Spain

35 Institute of Geography and Geoecology, Karlsruhe Institute of Technology, 76131 Karlsruhe, Germany

36 South African Institute of Aquatic Biodiversity, Makhanda, 6139, South Africa

37 present address: Department of Forest Ecology and Management, Swedish University of Agricultural Sciences, 90183 Umeå, Sweden

38 Department of Ecology and Environmental Sciences, Palacký University Olomouc, 77900 Olomouc, Czech Republic

39 Global Change Research Institute of the Czech Academy of Sciences, 603 00 Brno, Czech Republic

40 Environmental Research Institute, University of Highlands and Islands (UHI), Thurso KW14 7JD, Scotland, UK

41 Department of General and Applied Hydrobiology, Sofia University "St. Kliment Ohridski", 1164 Sofia, Bulgaria

42 Chemical Analytics and Biogeochemistry, Leibniz-Institute of Freshwater Ecology and Inland Fisheries, 12587 Berlin, Germany

43 present address: Groupe de Recherche Interuniversitaire en Limnologie, Département des Sciences Biologiques, Université du Québec à Montréal, Montréal H3C 3J7, Canada

*Corresponding author: Katrin Attermeyer (katrin.attermeyer@univie.ac.at)

Author order except first, second, and last author was computed randomly

Supplementary Tables

The supplementary contains a total of 4 additional tables. Supplementary Table 1 shows the descriptive parameters for each sampling site and Supplementary Table 2 lists the instruments for measuring temperature, conductivity, pH, oxygen, and discharge. Supplementary Table 3 shows median CO_2 fluxes for day and night together with the interquartile ranges for all stream sites and sampling periods and Supplementary Table 4 displays upscaled annual CO_2 fluxes from 14 European streams.

Supplementary Figures

The supplementary contains a total of 8 additional figures. Supplementary Figure 1 shows a map of the sampling sites in Europe with the labels given to each team participating in the EuroRun project and Supplementary Figure 2 gives impressions from the workshop in Sweden. Supplementary Figure 3 shows our measured CO_2 fluxes in comparison to the ones modelled in Hotchkiss et al. (2015). Supplementary Figure 4 displays the absolute changes of CO_2 fluxes from day to night related to different catchment and hydromorphological variables and Supplementary Figure 5 illustrates the changes of all measured and calculated biogeochemical parameters from day and night similar to Figure 1a in the manuscript. Supplementary Figure 6 shows the absolute changes of CO_2 fluxes from day to night separated by Strahler stream order and sampling period. Supplementary Figure 7 shows the diel CO_2 dynamics in the water of a Swedish agricultural stream from Wallin et al. (2020) and Supplementary Figure 8 diel CO_2 dynamics in the water of four selected streams from Bodmer et al. (2016).

Supplementary Methods

1) Organizational framework and study sites

This study was organized in the framework of the collaborative EuroRun project (described in Bodmer et al. (2019) [1]), uniting 46 mostly early career researchers in 16 teams distributed across 11 European countries. A flux chamber and CO_2 sensor were provided to each team, the measurement procedure and the data analysis were demonstrated to one lead representative from each team during a workshop and a detailed written protocol was provided to each team describing each step of the sampling procedure (Supplementary Hand out protocol, Supplementary Fig. S2).

In total, 34 stream sites (Fig. S1) were visited every three months during a specified two weeks' time frame except for 11 streams in January that were frozen during the sampling weeks (Table S3). Each team selected one to three sites with different dominant land uses (i.e., forest and/or agriculture) and a wide range of hydrological and watershed characteristics (Table S1). The stream order of the selected streams ranged between 1 up to 6, the wetted stream width between 1.0 to 22.3 m, mean depth between 0.11 to 1.99 m, and discharge from 0.01 to 6.32 $m^3 s^{-1}$. More details about the study sites, morphological, and biogeochemical parameters can be found in Table S1 and a table uploaded in figshare at http://doi.org/10.6084/m9.figshare.12717188.

Figure S1. Map of EuroRun sampling sites. Each dot represents one sampling site and the label indicates the team acronyms used for identifying study sites.

Table S1. Stream sampling sites included in this study and their descriptive parameters for the stream, catchment, and geology (na means not available).

Stream ID	Strahler stream order	Catchment area until endpoint of investigated stream reach (km^2)	Percentage of different land use within the catchment until endpoint of investigated stream reach forest/agriculture/urban/others				Predominant geology of the area	GPS coordinates (after WGS84)	Altitude (m above sea level)
AUT1_1	3	11.1	83	17	0	0	Sedimentary rocks	47°52′8.71″N / 15°0′2.63″E	648
AUT1_2	4	50.4	84	3	0	14	Sedimentary rocks	47°48′2.78″N / 14°57′2.13″E	542
AUT2_1	1	3.4	33	6	1	60	Sedimentary rocks	47°22'57.2"N / 11°44'34.4"E	539
AUT2_2	4	40.5	26	6	0	68	Metamorphic rocks	46°56'30.7"N / 12°03'21.2"E	1560
AUT2_3	1	0.7	5	60	16	19	Metamorphic rocks	47°15'34.3"N / 11°17'15.7"E	590
BGR1_1	5	1084.6	66	23	3	8	Metamorphic rocks	42°33'29.41"N / 23°25'22.98"E	638
BGR1_2	5	397.5	55	42	3	0	Igneous rocks	42°24′56.4″N / 23°31′44.8″E	838
CZE1_1	3	161.4	33	65	2	0	Sedimentary rocks	49°39´31,67″N 17°24´35,67″E	300
CZE1_2	4	447.8	32	64	4	0	Sediments	49°38´30,52″N 17°14´40,33″E	235
DEU1_1	4	643.0	60	29	3	8	Sediments	53°00'11.4"N / 12°54'12.1"E	39
DEU1_2	2	na	na	na	na	na	Sediments	53°06'05.2"N / 13°06'07.9"E	56
DEU2_1	3	54.8	95	0	5	0	Sedimentary rocks	49°14'14.96"N / 7°54'8.20"E	217
DEU2_2	4	145.6	95	0	5	0	Sedimentary rocks	49°21'54.972"N / 8°2'7.98"E	174
ESP1_1	3	24.1	35	45	20	0	Sedimentary rocks	42°04'50.6"N / 2°18'31.4"E	604
ESP1_2	5	172.3	80	5	15	0	Sedimentary rocks	42°15'29.9"N / 2°09'52.2"E	875
ESP1_3	4	59.8	50	30	20	0	Sedimentary rocks	42°10'38.0"N / 2°44'14.5"E	136
ESP2_1	4	71.4	85	5	10	0	Sedimentary rocks	42°19'09.7"N / 2°46'52.6"E	168
ESP2_2	6	189.5	30	40	30	0	Sedimentary rocks	42°13'08.2"N / 2°33'45.8"E	228
ESP2_3	2	32.9	5	85	10	0	Sedimentary rocks	42°05'46.2"N / 2°48'58.4"E	93
FRA1_1	3	222.6	56	43	2	0	Igneous rocks	45°55′46.5″N / 4°32′57.66″E	261
FRA1_2	4	266.4	65	28	2	5	Sedimentary rocks	45°55′6.9″N / 5°23′40.14″E	261
GBR1_1	3	81.0	23	1	0	77	Metamorphic rocks	58°25'01.9"N / 3°52'47.9"W	74
GBR1_2	3	50.9	22	0	0	78	Metamorphic rocks	58°25'31.6"N / 3°56'13.7"W	104
GBR2_1	2	8.4	100	0	0	0	Sedimentary rocks	50°48'07.3"N / 1°39'50.2"W	54
GBR2_2	4	382.2	0	100	0	0	Sedimentary rocks	50°40'44.9"N / 2°10'52.0"W	9
IRL1_1	3	4.6	32	0	0	68	Metamorphic rocks	53°58' 55.6"N / 9°34' 05.3"W	25
IRL1_2	4	30.4	17	4	0	79	Metamorphic rocks	53°59'18.6"N / 9°34'29.0"W	33
ITA1_1	4	118.9	38	49	4	9	Sedimentary rocks	44°43'37.54"N / 7°25'45.14"E	263
ITA1_2	4	157.8	44	0	2	55	Metamorphic rocks	44°48'42.02"N / 7°11'22.70"E	575
PRT1_1	2	62.9	56	42	1	0	Metamorphic rocks	41°37'51.71"N / 8°33'50.97"W	130
PRT1_2	2	15.4	40	58	2	0	Igneous rocks	41°34'6.21"N / 8°36'4.71"W	27
SWE1_1	4	104.2	68	16	1	15	Metamorphic rocks	63°55'12.55"N / 20°11'49.10"E	67
SWE2_1	1	23.3	94	5	1	0	Igneous rocks	60°00'40.9"N / 17°50'56.6"E	13
SWE2_2	3	27.5	31	61	0	8	Metamorphic rocks	59°42'59.0"N / 17°08'43.0"E	19

Table S2. Multiparameter probes and flowmeters used during the samplings by each team.

Team ID	Physical and chemical measurement instrument	Discharge instrument
AUT1	Portable three channel multi meter 3430, WTW GmbH, Germany	OTT MF pro; OTT Hydromet, Germany
AUT2	Portable three channel multi meter 3430, WTW GmbH, Germany	OTT MF pro; OTT Hydromet, Germany
BGR1	Portable handheld meters series 330i, WTW GmbH, Germany	Model 2100, Swoffer instruments Inc, USA
CZE1	EC: DiST 3 EC tester, Hanna Instruments, USA; DO, T: HI 9147 Dissolved oxygen meter, Hanna Instruments, USA	Flo-mate model 2000, Marsh-McBirney Inc., USA
DEU1	AquaTROLL 400, In-situ, USA	OTTO, Germany
DEU2	Portable three channel multi meter 3430 IDS, WTW GmbH, Germany	OTT MF pro, OTT Hydromet, Germany
ESP1	EC, T, pH: Portable hand-held probes multiline 3310, WTW GmbH, Germany; DO: ProODO Handheld, YSI, USA	Acoustic Doppler Velocimeter FlowTracker, SonTek, USA or P670 flowmeter, DOSTMANN electronic, GmbH, Germany
ESP2	EC, T, pH: Portable hand-held probes multiline 3310, WTW GmbH, Germany; DO: ProODO Handheld, YSI, USA	Acoustic Doppler Velocimeter FlowTracker, SonTek, USA or P670 flowmeter, DOSTMANN electronic, GmbH, Germany
FRA1	EC: Hach d40, Hach, USA; pH, DO, T: Od14, Hach, USA	Flo-mate model 2000, Marsh-McBirney Inc., USA
GBR1	YSI 556 MPS - multi probe system (Model: Pro 2030), Environmental (Company), USA	Water level gauge and Manning`s equation [2,3]
GBR2	YSI 556 MPS - multi probe system (Model: Pro 2030), Environmental (Company), USA	Geopacks, UK
IRL1	Quanta – Hydrolab, Texas, USA	OTT Sensa Z300, Germany
ITA1	Quanta – Hydrolab, Texas, USA	Hydro-bios Kiel, Mod RHCM Idromar
PRT1	WTW Multi 340i, WTW GmbH, Germany	Geopacks “Flowmeter 1”, UK
SWE1	EC: Konduktometer CG 857 (Schott Geräte GmbH); DO: OxyGuard Handy Delta Portable DO meter; pH: Mettler Toledo 1120	Argonaut Acoustic Doppler Velocimeter, SonTek, USA
SWE2	EC, pH: HI991300, Hanna Instruments, USA; DO, T: YSI ProODO Handheld, YSI, USA	µP-TAD, Höntzsch Instruments, Waiblingen, Germany or bucket when flow too low to use flowmeter

EC: Electrical conductivity; DO: Dissolved oxygen; T: Temperature

2) Measurements of pCO_2 and geological information extraction

The partial pressure of CO_2 (pCO_2) in the water was determined in the majority of the teams through the chamber equilibration method, which measures surface water concentrations after equilibration of pCO_2 in the headspace of the chamber with the surface water [4]. The method is based on the assumption that after the chamber headspace has equilibrated with the water, the measured pCO_2 in the chamber headspace represents the surface water pCO_2. Alternatively, water pCO_2 was measured with an Infrared Gas Analyzer (IRGA) (teams ESP1/2, SWE2), a gas chromatograph (Shimadzu GC-14B equipped with autosampler AOC 5000, FID, Shimadzu, Kyoto, Japan; team DEU1) or a handheld nondispersive infrared CO_2 sensor (CARBOCAP GM70, Vaisala, Helsinki, Finland) with a sensor probe (CARBOCAP GMP220) enclosed in a semipermeable polytetrafluoroethylene membrane, following the methods established by Johnson et al. (2010) [5] (team SWE1) and calibrated against reference gas mixtures as described in Klaus et al. (2019) [6].

The samples for IRGA for the team SWE2 were prepared according to the headspace equilibrium method [7]. With a syringe, 30 mL of water was taken right below the surface followed by adding 30 mL of ambient air to create a headspace. Triplicates were taken at day- and night-time. Equilibrated gas samples were analyzed on a portable infrared gas analyzer (IRGA, EGM-4) within 5 min of sampling. The pCO_2 was calculated according to Weiss (1974) [8] using the appropriate Henry's constant after correcting for temperature, atmospheric pressure, and the amount of ambient air CO_2 added. The teams ESP1/2 coupled the IRGA to a membrane contactor (MiniModule, Liqui-Cel, USA). The water was circulated via gravity through the contactor at 300 mL min^{-1}, and the equilibrated gas was continuously recirculated into the infrared gas analyzer for instantaneous pCO_2 measurements.

Geological information of the sites were obtained from the EuroGeoSurveys' European Geological Data Infrastructure web (EGDIS (EuroGeoSurveys' European Geological Data Infrastructure) [9] available at: http://www.europe-geology.eu/onshore-geology/geological-map/.) using their geographical coordinates. For each site, we retrieved information on (i) surface lithology according to the Infrastructure for Spatial Information in the European Community (INSPIRE) [10], and (ii) predominant petrology according to the International Geological Map of Europe and Adjacent Areas (IGME 5000) [11]. Based on this information, we then defined the predominant geology of the area for each site by assigning them one of the four main rock types (igneous rocks, metamorphic rocks, sedimentary rocks and sediments).

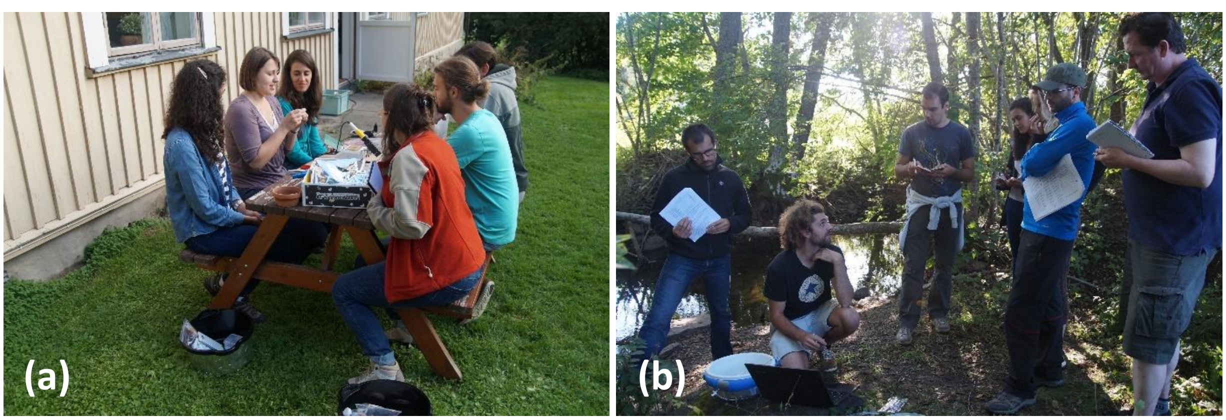

Figure S2. The workshop participants learn how to solder and repair the CO_2 sensor at Erken Laboratory from Uppsala University located at Lake Erken in Norrtälje, Sweden (a) and the measurement procedure at a stream nearby (b) in September 2016.

3) Temporal upscaling from hourly to annual areal CO_2 fluxes

To evaluate the impact of the differences between day- and night-time CO_2 fluxes in streams on an annual scale, we upscaled our data in two ways. Firstly, the median values for the hourly CO_2 fluxes from day-time in each sampling period were taken and multiplied by 24 hours and integrated over a 3-month period around the sampling. Secondly, the median values for the hourly CO_2 fluxes from day-time were multiplied by the hours of the day from sunrise to sunset and from night-time by the hours from sunset to sunrise, respectively. The times of sunrise and sunset for each day and location were retrieved with the package "suncalc" in R [12]. Finally, the differences in the annual areal CO_2 fluxes considering only day-time fluxes to day- and night-time fluxes were calculated and expressed in % relative to day-time fluxes to compare the extent of missing information when only measuring during day-time. Only stream sites with data for all four seasons were taken into account which limits these calculations to 14 sites (Table S4). This upscaling represents a preliminary evaluation on the underestimation of fluvial CO_2 fluxes when nights are not considered. It is just based on four days throughout one year and one fixed time slot during day-time and during night-time but should serve as a first orientation for future studies.

Supplementary Results

Table S3. Median CO_2 fluxes (in mmol m^{-2} h^{-1}) and interquartile ranges [IQR] for all streams and sampling periods. Changes in CO_2 fluxes from day to night are highlighted with color (light red: median CO_2 flux increases from day to night; dark red: increases from negative or zero fluxes to positive CO_2 fluxes; blue: median CO_2 flux decreases from day to night; yellow: no change in median CO_2 fluxes). Sites with na indicate not enough replicates (sample size < 3) for either day or night available from the floating chamber runs and were, hence, excluded from all comparisons.

Country	Stream ID	October		January		April		July	
		Day	Night	Day	Night	Day	Night	Day	Night
Austria	AUT1_1	7.2 [5.9, 7.4]	12.9 [9.0, 13.3]	1.7 [1.5, 1.7]	2 [1.8, 2.1]	0.6 [0.6, 0.7]	1.6 [1.6, 1.7]	0.6 [0.5, 0.8]	1.6 [1.3, 1.7]
Austria	AUT1_2	1.5 [1.4, 1.6]	1.4 [1.1, 1.6]	1.4 [1.4, 1.4]	2.1 [1.9, 2.2]	1.1 [1.0, 1.2]	1.6 [1.5, 1.8]	0.8 [0.7, 1.0]	1 [0.9, 1.2]
Austria	AUT2_1	4.2 [3.5, 9.7]	6.9 [6.3, 7.4]	8.4 [6.1, 8.7]	8.9 [7.6, 9.2]	6.8 [6.7, 7.9]	10.8 [10.6, 13.5]	8.5 [7.8, 10.2]	11.8 [10.2, 12.1]
Austria	AUT2_2	0 [-0.3, 0]	0.2 [0, 0.3]	ice	ice	0 [0, 0]	0.3 [0.2, 0.3]	0 [0, 0]	-0.1 [-0.7, 0.5]
Austria	AUT2_3	0 [0, 0]	0.8 [0.7, 0.9]	ice	ice	-0.6 [-0.7, -0.6]	0.7 [0.7, 0.7]	0 [0, 0.3]	0.6 [0.6, 1.3]
Bulgaria	BGR1_1	na	na	ice	ice	na	na	0.2 [0.1, 0.3]	0.5 [0.4, 0.5]
Bulgaria	BGR1_2	-0.9 [-1, -0.8]	0.8 [0.3, 1]	ice	ice	-0.9 [-1.3, -0.9]	2.4 [2.3, 2.9]	na	na
Czech Republic	CZE1_1	1 [0.7, 1.2]	3.4 [3.2, 3.5]	ice	ice	-2.7 [-3.4, -2.4]	2.9 [2.8, 3]	0.6 [0.6, 0.6]	3.6 [3.4, 3.7]
Czech Republic	CZE1_2	2.7 [2.2, 3.6]	4 [3.2, 4.1]	ice	ice	2.1 [2, 2.2]	7.4 [6.7, 7.6]	1.2 [1.2, 1.4]	2.4 [2.3, 3.2]
Germany	DEU1_1	3.3 [3.2, 3.5]	3.9 [3, 4.8]	2.5 [2.1, 2.7]	3.2 [2.6, 3.8]	2.5 [2.5, 3]	2.6 [2.2, 2.7]	3 [2.5, 3.2]	2.2 [2, 2.4]
Germany	DEU1_2	na	na	6.4 [3, 8.4]	3 [1.9, 11]	3.1 [3, 3.3]	5 [4.1, 5.2]	6.8 [6, 6.9]	8.8 [7.3, 10.8]
Germany	DEU2_1	3.6 [3.5, 3.8]	5.1 [4.8, 5.6]	3 [2.9, 3]	3.8 [3.6, 3.8]	1.6 [1.6, 1.6]	4 [3.9, 4.1]	3 [2.7, 3]	3.7 [3.3, 3.7]
Germany	DEU2_2	1.8 [1.7, 1.9]	2.5 [2.4, 2.9]	1 [1, 1.1]	1.9 [1.8, 2]	0.7 [0.7, 0.8]	3 [3, 3.1]	2.8 [2.8, 2.8]	4.1 [4, 4.1]
Spain	ESP1_1	-0.4 [-0.5, 0.1]	-0.1 [-0.4, 0.3]	0.2 [0.1, 0.3]	0.3 [0.2, 0.4]	0.4 [0.4, 0.4]	0.5 [0.4, 0.6]	0.4 [0.3, 1.1]	0.4 [0.4, 0.5]
Spain	ESP1_2	na	na	-0.4 [-0.5, -0.4]	1.1 [1.0, 1.2]	na	na	na	na
Spain	ESP1_3	2.8 [2.5, 2.9]	4 [3.8, 4.1]	3.1 [2.5, 3.8]	3.4 [3.2, 3.4]	1.2 [1.1, 1.7]	2.7 [2.0, 6.7]	1.8 [1.4, 2.4]	1.4 [1.4, 2.1]
Spain	ESP2_1	1.4 [1.3, 1.4]	1.2 [1.2, 1.3]	0.8 [0.8, 1.0]	1.1 [1.0, 1.2]	0.6 [0.6, 0.8]	2.4 [1.5, 3.4]	1.1 [0.9, 1.3]	1.5 [1.2, 1.9]
Spain	ESP2_2	0.7 [0.6, 0.8]	0.8 [0.7, 0.8]	0.5 [0.3, 0.7]	0.8 [0.7, 0.8]	na	na	na	na
Spain	ESP2_3	0.6 [0.5, 0.7]	1.8 [1.7, 2.5]	2.6 [2.5, 3.1]	0.9 [0.8, 1.1]	1.2 [1.2, 1.4]	2.4 [1.6, 2.7]	1.5 [1.3, 2.1]	2.5 [2.2, 2.9]
France	FRA1_1	1.2 [0.9, 1.2]	2.6 [1.4, 3]	na	na	-0.6 [-0.6, -0.5]	2.3 [2.2, 2.5]	0.4 [0.3, 0.4]	0.9 [0.7, 0.9]
France	FRA1_2	na	na	2 [1.8, 2.1]	3 [2.4, 3.4]	6 [4.6, 6.2]	3.7 [3.1, 4]	0.5 [0.4, 0.5]	4.1 [2.8, 4.9]
Great Britain	GBR1_1	-0.4 [-0.4, -0.3]	-0.3 [-0.3, -0.2]	ice	ice	-0.2 [-0.3, -0.2]	-0.2 [-0.2, -0.2]	1.2 [0.9, 1.2]	1.4 [1.2, 1.5]
Great Britain	GBR1_2	na	na	ice	ice	0.5 [0.3, 0.4]	0.5 [0.4, 0.5]	2.3 [2.2, 2.4]	1.8 [1.6, 1.9]
Great Britain	GBR2_1	3.2 [3, 3.3]	2.3 [1.8, 2.4]	4.9 [4, 5.2]	5.8 [5.1, 5.9]	1.9 [1.6, 1.9]	2.7 [2.6, 2.9]	4.9 [4.7, 5.3]	3.2 [2.9, 3.3]

Great Britain	GBR2_2	2 [1.8, 2.1]	1 [0.9, 1.1]	3.6 [2.9, 3.6]	3.9 [3.7, 4.5]	1.5 [1.4, 1.5]	1.7 [1.4, 2.3]	2.2 [2.1, 2.5]	1.5 [1.1, 1.6]
Ireland	IRL1_1	0.4 [0.4, 0.7]	1.3 [1.3, 1.6]	0.5 [0.5, 0.6]	0.9 [0.8, 0.9]	0.4 [0.4, 0.5]	0.7 [0.6, 0.8]	na	na
Ireland	IRL1_2	0.6 [0.5, 0.7]	1.2 [1.0, 1.4]	0.5 [0.4, 0.5]	0.6 [0.4, 0.8]	na	na	na	na
Italy	ITA1_1	13 [10.4, 13]	13.3 [8.7, 13.8]	19.9 [19.4, 23.8]	25.6 [22, 28.2]	16.8 [13.6, 19.6]	18 [14.2, 18.1]	13 [12.5, 13.8]	10.9 [9, 10.9]
Italy	ITA1_2	na	na	-1 [-1.1, -0.9]	0.6 [0.6, 0.7]	na	na	0 [0, 0.3]	0.5 [0.3, 0.9]
Portugal	PRT1_1	0.8 [0.8, 2.2]	0.9 [0.8, 0.9]	na	na	3.2 [2.7, 5.3]	7 [5.9, 7.9]	0.9 [0.8, 1.5]	0.8 [0.8, 0.8]
Portugal	PRT1_2	4.8 [4.5, 5.1]	4.5 [4.2, 5.1]	14.2 [13.4, 17.6]	20.5 [19.3, 20.9]	6.1 [4.2, 6.7]	7.7 [6.8, 18.9]	7.6 [7.3, 7.7]	11.8 [9.6, 12.4]
Sweden	SWE1_1	3.3 [2.7, 3.4]	3.1 [3.0, 4.6]	ice	ice	6.3 [5.2, 7.5]	1.8 [1.8, 3.9]	1.4 [1.2, 1.8]	1.7 [1.7, 2.4]
Sweden	SWE2_1	0.8 [0.7, 0.8]	1 [0.8, 1.2]	ice	ice	3.2 [3.1, 3.3]	2.4 [1.7, 2.8]	1 [0.5, 1.0]	0.6 [0.4, 2.5]
Sweden	SWE2_2	1.5 [0.8, 1.6]	1.5 [1.2, 1.7]	ice	ice	0.9 [0.8, 1.0]	1.3 [1.2, 1.6]	1.6 [1.5, 1.6]	1.3 [1.2, 1.4]

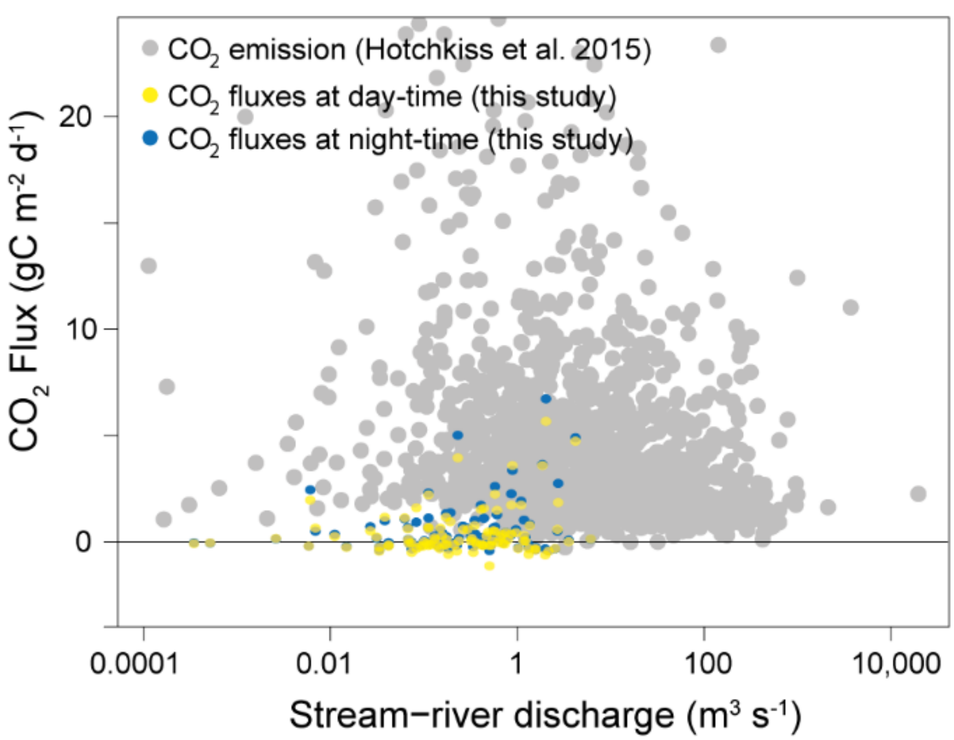

Figure S3. Directly measured CO_2 flux data from this study (in gC m^{-2} d^{-1}; yellow for CO_2 flux during day-time and blue for night-time) in comparison to the CO_2 fluxes based on calculated pCO_2 and modelled gas exchange velocity in Hotchkiss et al. (2015) [13]. The fluxes are plotted against discharge ranging from 0.0001 to >10,000 m^3 s^{-1}.

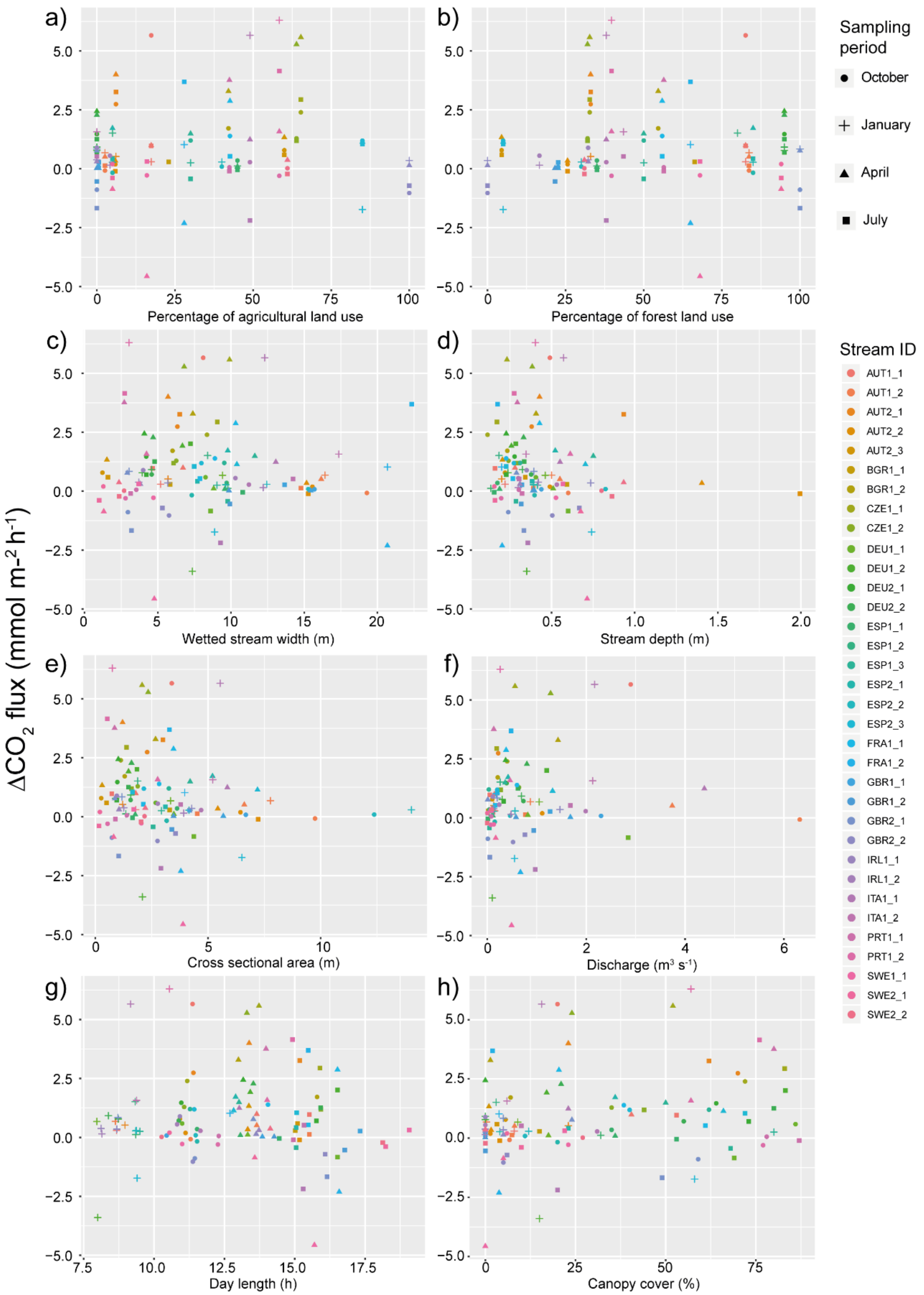

Figure S4. The absolute changes of CO_2 fluxes (ΔCO_2 flux) from day to night related to different catchment and hydromorphological variables. Different symbols distinguish different sampling periods and the different colors display each sampling site.

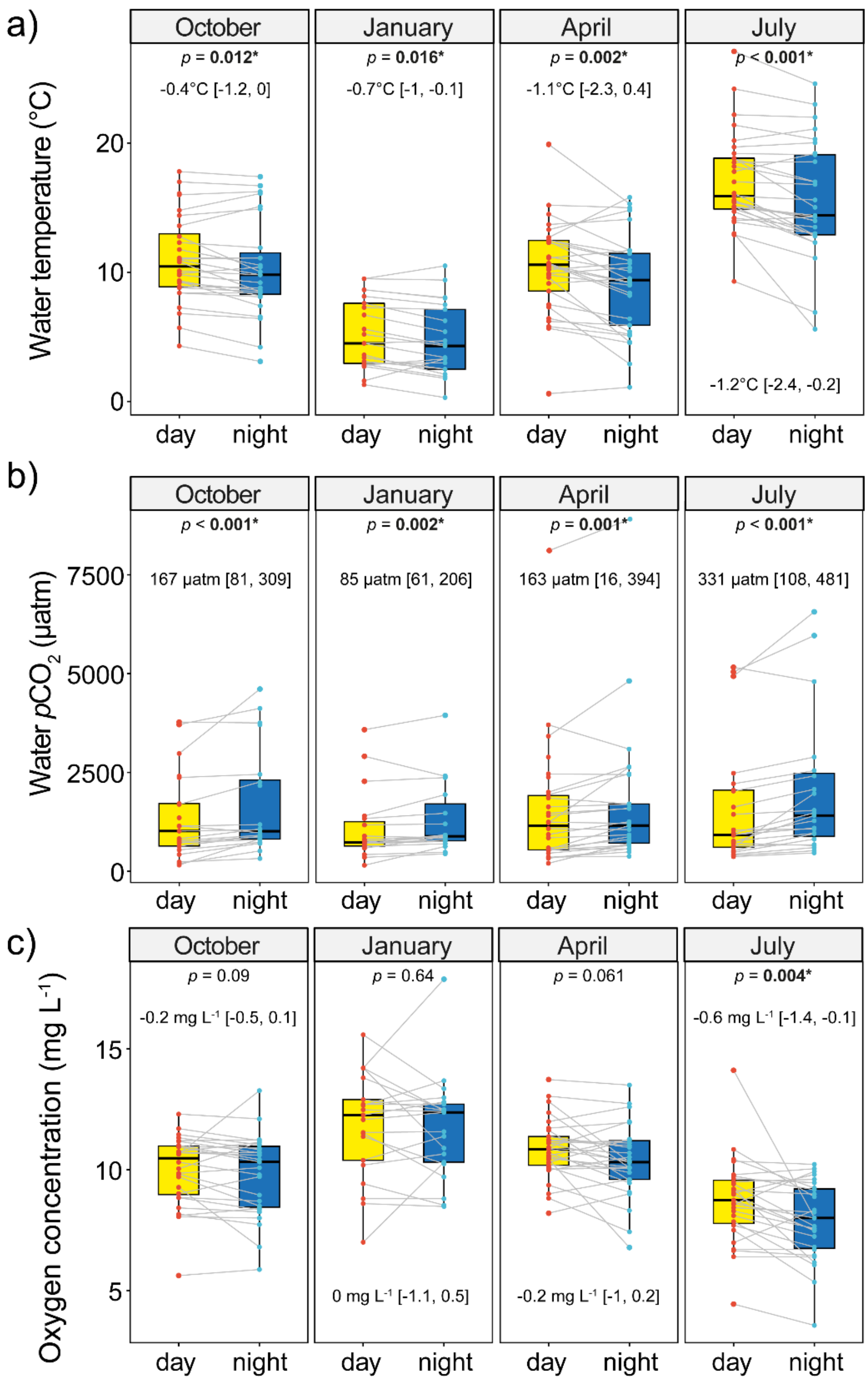
a)
October
January
April
July
p = 0.012*
-0.4°C [-1.2, 0]
p = 0.016*
-0.7°C [-1, -0.1]
p = 0.002*
-1.1°C [-2.3, 0.4]
p < 0.001*
-1.2°C [-2.4, -0.2]
Water temperature (°C)
0
10
20
day
night
b)
p < 0.001*
167 µatm [81, 309]
p = 0.002*
85 µatm [61, 206]
p = 0.001*
163 µatm [16, 394]
p < 0.001*
331 µatm [108, 481]
Water pCO2 (µatm)
0
2500
5000
7500
c)
p = 0.09
-0.2 mg L-1 [-0.5, 0.1]
p = 0.64
0 mg L-1 [-1.1, 0.5]
p = 0.061
-0.2 mg L-1 [-1, 0.2]
p = 0.004*
-0.6 mg L-1 [-1.4, -0.1]
Oxygen concentration (mg L-1)
5
10
15

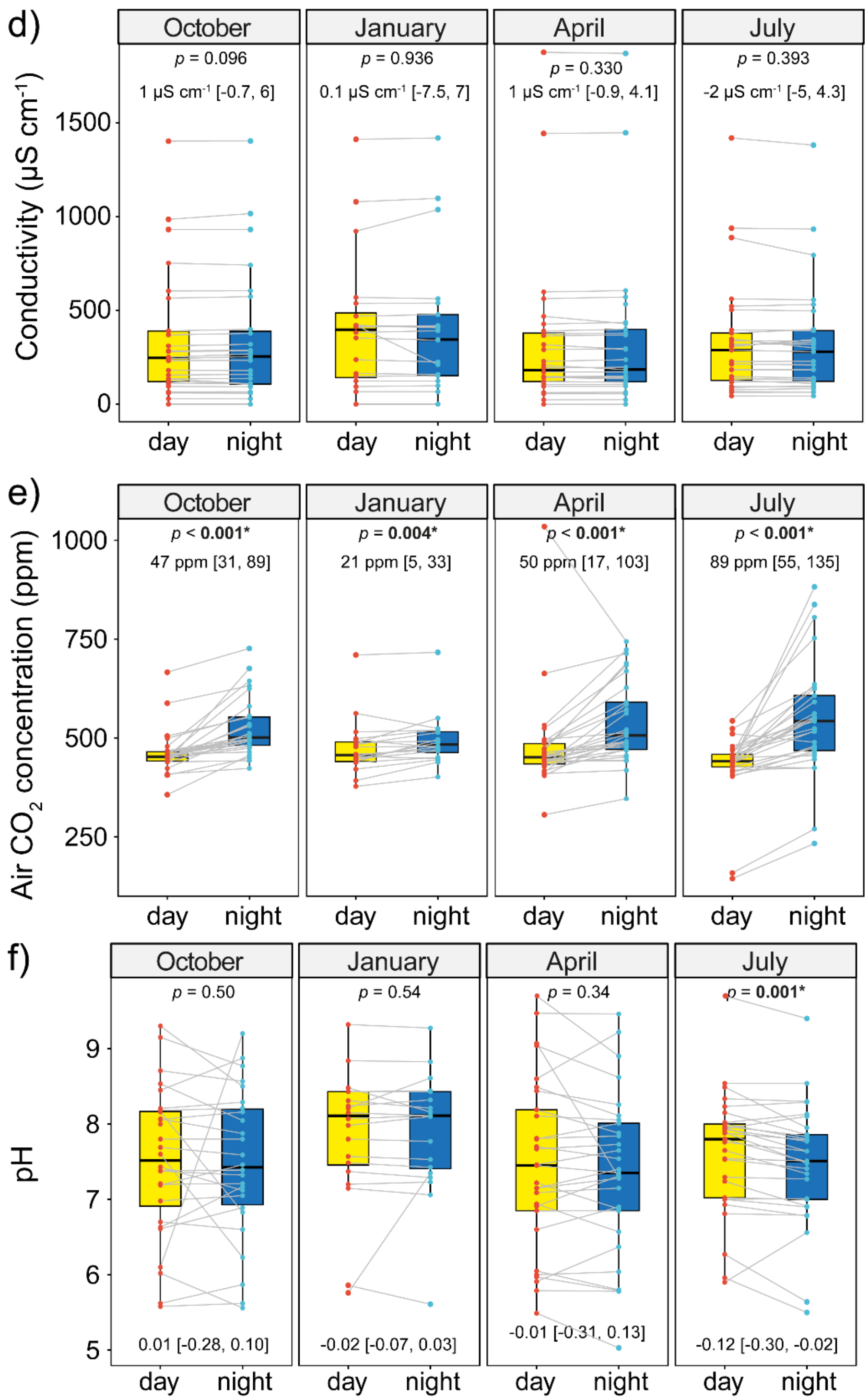
d)
October
January
April
July
p = 0.096
1 μS cm-1 [-0.7, 6]
p = 0.936
0.1 μS cm-1 [-7.5, 7]
p = 0.330
1 μS cm-1 [-0.9, 4.1]
p = 0.393
-2 μS cm-1 [-5, 4.3]
Conductivity (μS cm-1)
0
500
1000
1500
day
night
e)
p < 0.001*
47 ppm [31, 89]
p = 0.004*
21 ppm [5, 33]
p < 0.001*
50 ppm [17, 103]
p < 0.001*
89 ppm [55, 135]
Air CO2 concentration (ppm)
250
500
750
1000
f)
p = 0.50
0.01 [-0.28, 0.10]
p = 0.54
-0.02 [-0.07, 0.03]
p = 0.34
-0.01 [-0.31, 0.13]
p = 0.001*
-0.12 [-0.30, -0.02]
pH
5
6
7
8
9

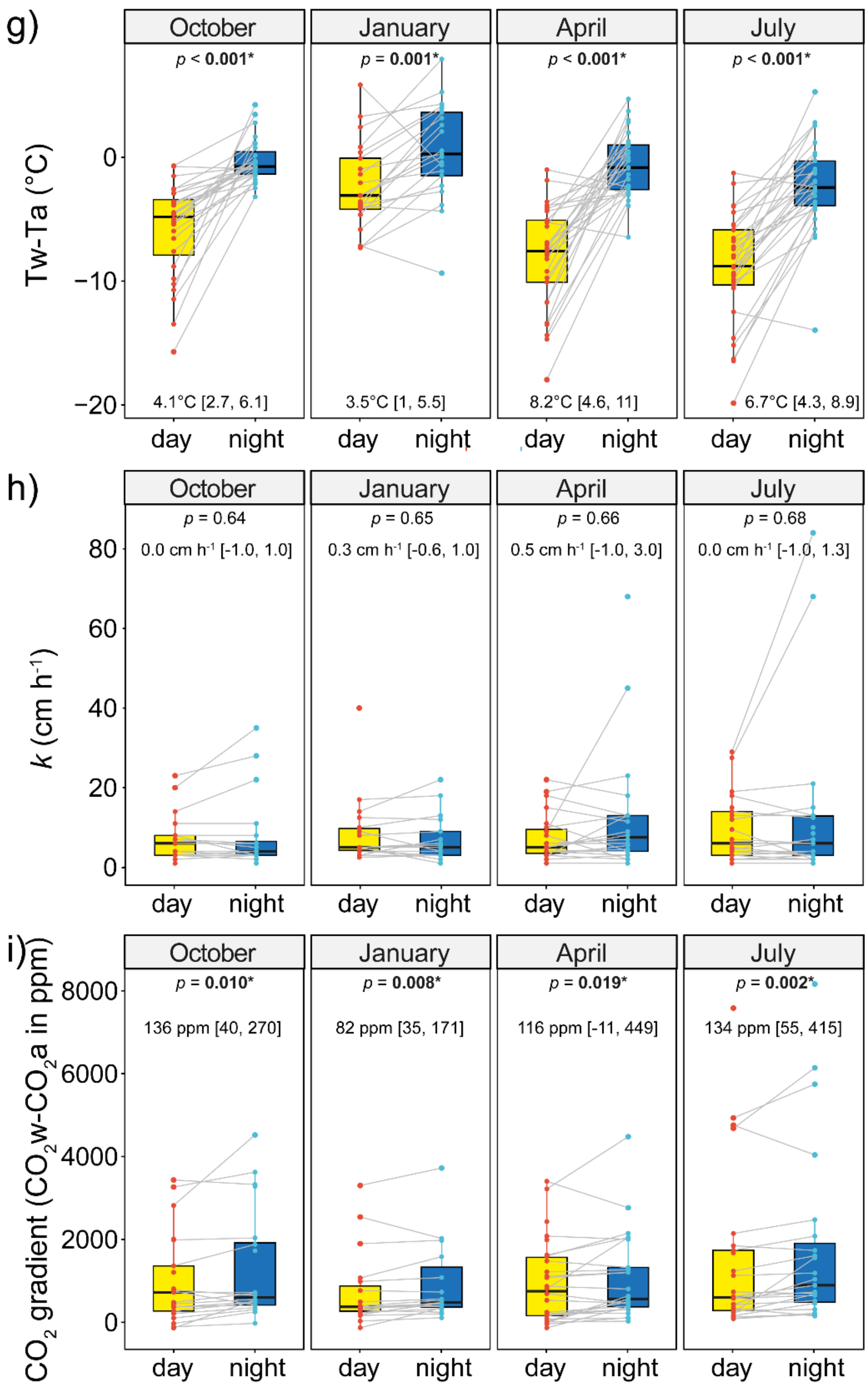

Figure S5. Physical and chemical parameters measured at day- and night-time for each sampling period and the changes for each site indicated by a line as a visual help. The parameters include a) water temperature (°C), b) water pCO_2 (µatm), c) oxygen concentration (mg L^{-1}), d) conductivity (µS cm^{-1}), e) air CO_2 concentration (ppm), f) pH, g) a proxy for heat flux as temperature in the water minus temperature in the air (°C), h) gas transfer velocity *k* at *in situ* temperature (cm h^{-1}), and i) the CO_2 gradient calculated as pCO_2 in the water minus CO_2 in the air (ppm). The boxplots visualize the median of all stream sites (line), the first and third quartiles (hinges), and the 1.5 * inter-quartile ranges (IQR) (whiskers). The *p* values are given for the Wilcoxon signed rank test as well as the median value of the change [IQR] for each sampling period.

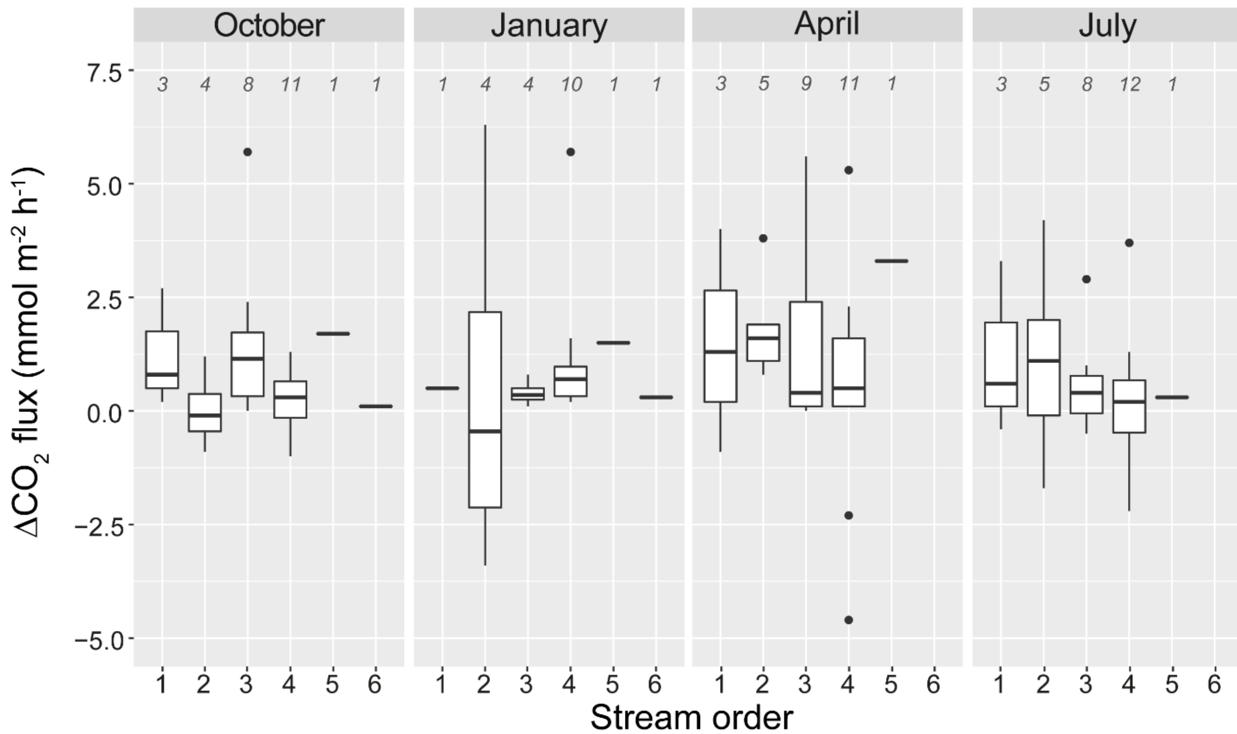

Figure S6. The absolute changes of CO_2 fluxes (ΔCO_2 flux) from day to night separated by Strahler stream order and sampling period. The sample sizes for each Strahler stream order and sampling period is given on top of the graph in gray and italics.

Table S4. Upscaled annual CO_2 fluxes from 14 European streams where a full dataset was available for all sampling periods to assess the influence of only day-time measurements versus inclusion of day- and night-time measurements of CO_2 fluxes.

Stream ID	**Annual CO_2 flux (mol m^{-2} y^{-1})**		**Difference (day+night minus only day)**		
	Only day	**Day and night**	**mol m^{-2} y^{-1}**	**mgC m^{-2} y^{-1}**	**%**
AUT1_1	22.03	30.90	8.88	106.5	40
AUT1_2	10.34	11.75	1.41	16.9	14
AUT2_1	60.97	71.41	10.44	125.3	17
DEU1_1	24.81	25.94	1.14	13.6	5
DEU2_1	24.39	30.08	5.69	68.2	23
DEU2_2	13.96	19.21	5.25	63.0	38
ESP1_1	1.21	1.82	0.61	7.4	51
ESP1_3	19.53	22.37	2.83	34.0	14
ESP2_1	8.63	10.83	2.21	26.5	26
ESP2_3	13.00	14.20	1.20	14.4	9
GBR2_1	32.65	32.17	-0.49	-5.8	-1
GBR2_2	20.25	19.07	-1.18	-14.2	-6
ITA1_1	137.07	144.16	7.10	85.1	5
PRT1_2	71.34	84.21	12.87	154.4	18

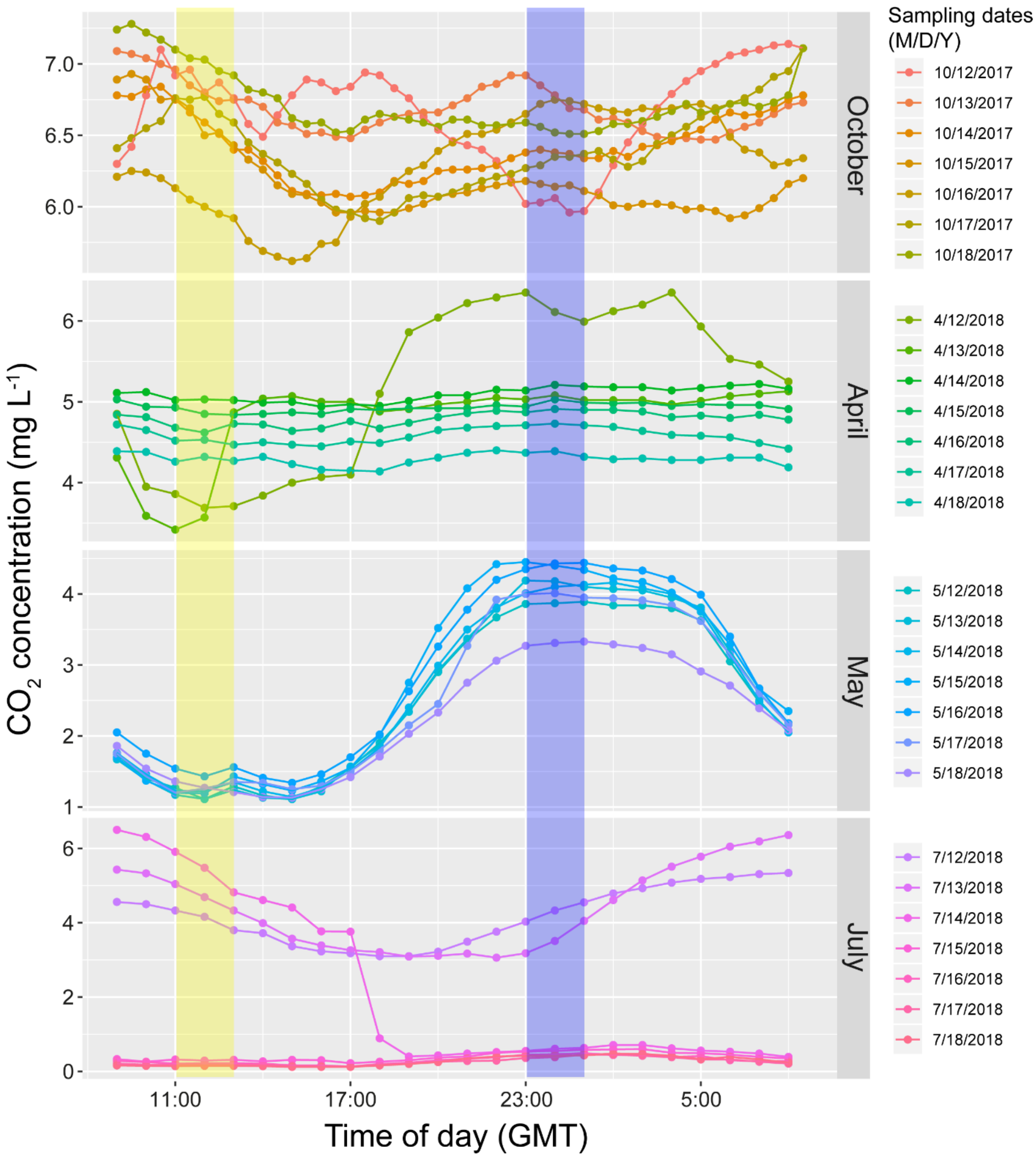

Figure S7. Diel CO_2 dynamics in the water of a Swedish agricultural stream from Wallin et al. (2020)[15], which is located close by the EuroRun site SWE2_2. The CO_2 concentration is shown over 24 hours for each day of one week in the month October, April, May (peak time of diel CO_2 concentration differences in this study) and July. The approximate sampling window chosen for this study (11:00 and 23:00 GMT) is highlighted in blue for the night and yellow for the day.

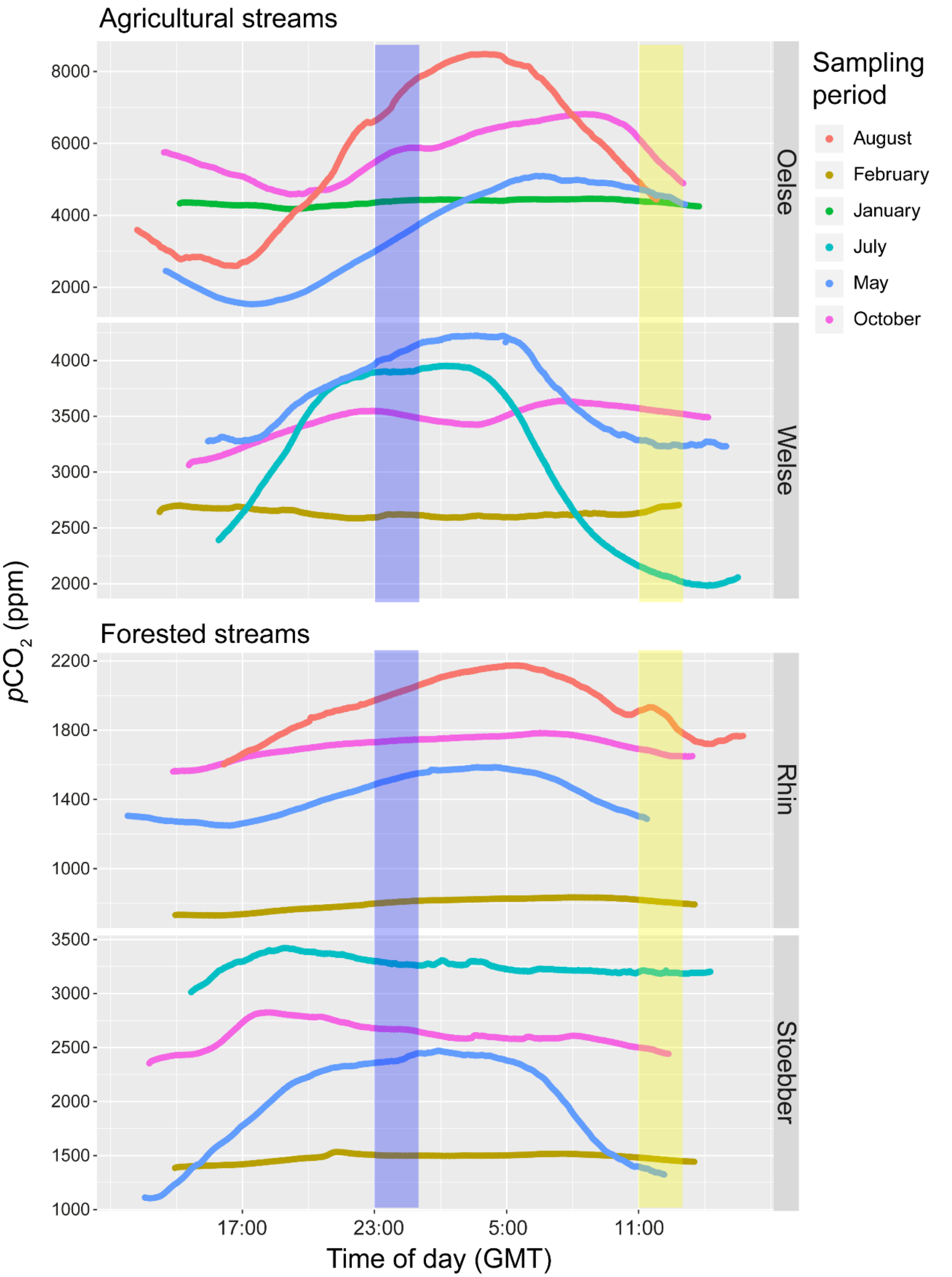

Figure S8. Diel CO_2 dynamics in the water of four selected streams from Bodmer et al. (2016)[14]. The streams have different dominated land uses and are located in Germany (more information please refer to the reference of Bodmer et al. (2016)). The CO_2 was measured over 24 hours in different months in 2013/2014 and the Rhin is a sampling site of EuroRun (DEU1_1). The approximate sampling window chosen for this study (11:00 and 23:00 GMT) is highlighted in blue for the night and yellow for the day.

References

1. Bodmer, P., Attermeyer, K., Pastor, A. & Catalán, N. Collaborative Projects: Unleashing Early Career Scientists' Power. *Trends Ecol. Evol.* **34**, 871–874 (2019).

2. Manning, R., Griffith, J. P., Pigot, T. F. & Vernon-Harcourt, L. F. On the flow of water in open channels and pipes. in *Transactions of the Institution of Civil Engineers of Ireland* 161–207 (1890).

3. Dingman, S. L. & Sharma, K. P. Statistical development and validation of discharge equations for natural channels. *J. Hydrol.* **199**, 13–35 (1997).

4. Bastviken, D., Sundgren, I., Natchimuthu, S., Reyier, H. & Gålfalk, M. Technical Note: Cost-efficient approaches to measure carbon dioxide (CO2) fluxes and concentrations in terrestrial and aquatic environments using mini loggers. *Biogeosciences* **12**, 3849–3859 (2015).

5. Johnson, M. S. *et al.* Direct and continuous measurement of dissolved carbon dioxide in freshwater aquatic systems—method and applications. *Ecohydrology* **3**, 68–78 (2010).

6. Klaus, M., Geibrink, E., Hotchkiss, E. R. & Karlsson, J. Listening to air–water gas exchange in running waters. *Limnol. Oceanogr. Methods* **17**, 395–414 (2019).

7. Sobek, S., Algesten, G., Bergström, A. K., Jansson, M. & Tranvik, L. J. The catchment and climate regulation of pCO2 in boreal lakes. *Glob. Chang. Biol.* **9**, 630–641 (2003).

8. Weiss, R. F. Carbon dioxide in water and seawater: The solubility of a non-ideal gas. *Mar. Chem.* **2**, 203–215 (1974).

9. EGDIS (EuroGeoSurveys' European Geological Data Infrastructure). Available at: http://www.europe-geology.eu/onshore-geology/geological-map/.

10. Laxton, J. L. Geological map fusion: OneGeology-Europe and INSPIRE. in *Integrated Environmental Modelling to Solve Real World Problems: Methods, Vision and Challenges* (eds. Riddick, A. T., Kessler, H. & Giles, J. R. A.) 147–160 (Geological Society Publishing House, 2017).

11. Asch, K. Geology without national boundaries - The 1:5 million international geological map of Europe and adjacent areas - IGME 5000. *Episodes* **29**, 39–42 (2006).

12. Agafonkin, V. & Thieurmel, B. suncalc: Compute Sun Position, Sunlight Phases, Moon Position and Lunar Phase. *R Packag. version 0.4* (2018).

13. Hotchkiss, E. R. *et al.* Sources of and processes controlling CO2 emissions change with the size of streams and rivers. *Nat. Geosci.* **8**, 696–699 (2015).

14. Bodmer, P., Heinz, M., Pusch, M., Singer, G. & Premke, K. Carbon dynamics and their link to dissolved organic matter quality across contrasting stream ecosystems. *Sci. Total Environ.* **553**, 574–586 (2016).

15. Wallin, M. B., Audet, J., Peacock, M., Sahlée, E. & Winterdahl, M. Carbon dioxide dynamics in an agricultural headwater stream driven by hydrology and primary production. *Biogeosciences* **17**, 2487–2498 (2020).